

Spring 2019

Acute Effects of Elevated pCO₂ and Hypoxia on Blue Rockfish (*Sebastes mystinus*) Gene Expression and Metabolic Enzyme Activity

Andrew Jacob Cline
California State University, Monterey Bay, acline@csumb.edu

Follow this and additional works at: https://digitalcommons.csumb.edu/sns_theses

Recommended Citation

Cline, Andrew Jacob, "Acute Effects of Elevated pCO₂ and Hypoxia on Blue Rockfish (*Sebastes mystinus*) Gene Expression and Metabolic Enzyme Activity" (2019). *SNS Master's Theses*. 39.
https://digitalcommons.csumb.edu/sns_theses/39

This Master's Thesis (Open Access) is brought to you for free and open access by the School of Natural Sciences at Digital Commons @ CSUMB. It has been accepted for inclusion in SNS Master's Theses by an authorized administrator of Digital Commons @ CSUMB. For more information, please contact digitalcommons@csumb.edu.

ACUTE EFFECTS OF ELEVATED PCO_2 AND HYPOXIA ON BLUE
ROCKFISH (*SEBASTES MYSTINUS*) GENE EXPRESSION AND
METABOLIC ENZYME ACTIVITY

A Thesis
Presented to the
Faculty of the
School of Natural Sciences
California State University Monterey Bay

In Partial Fulfillment
of the Requirements for the Degree
Master of Science
in
Applied Marine and Watershed Science

by
Andrew Jacob Cline

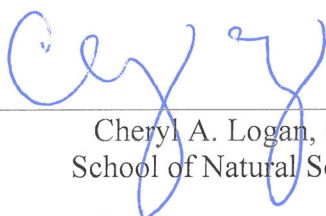
Spring 2019

CALIFORNIA STATE UNIVERSITY MONTEREY BAY

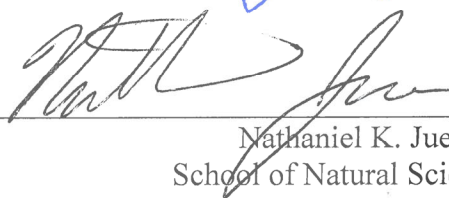
The Undersigned Faculty Committee Approves the

Thesis of Andrew Jacob Cline:

ACUTE EFFECTS OF ELEVATED PCO_2 AND HYPOXIA ON BLUE
ROCKFISH (*SEBASTES MYSTINUS*) GENE EXPRESSION AND
METABOLIC ENZYME ACTIVITY



Cheryl A. Logan, Chair
School of Natural Sciences



Nathaniel K. Jue
School of Natural Sciences



Scott L. Hamilton
Moss Landing Marine Laboratories, Moss Landing, CA

Approved by the Dean of Graduate Studies 

Kris Roney, Dean
Associate VP for Academic Programs and Dean of Undergraduate and Graduate Studies

21 May 2019
Approval Date

Copyright © 2019

by

Andrew Jacob Cline

All Rights Reserved

ABSTRACT

Acute Effects of Elevated $p\text{CO}_2$ and Hypoxia on Blue Rockfish (*Sebastes mystinus*) Gene Expression and Metabolic Enzyme Activity

by

Andrew Jacob Cline

Master of Science in Applied Marine and Watershed Science
California State University Monterey Bay, 2018

In the Northeast Pacific, seasonal upwelling periodically exposes nearshore organisms to elevated levels of $p\text{CO}_2$ and hypoxia. Upwelling is projected to intensify under climate change as more frequent and intense alongshore wind events bring deeper, more acidic and hypoxic seawater to shallower depths and into nearshore ecosystems. Previous work demonstrated that blue rockfish (*Sebastes mystinus*) are relatively tolerant to high levels of $p\text{CO}_2$ at multiple biological scales compared with copper rockfish (*S. caurinus*) following chronic exposure for multiple months. To investigate the tolerance of juvenile blue rockfish over shorter, more ecologically relevant periods, I measured changes in muscle tissue gene expression at 12 h, 24 h and two weeks of exposure to elevated $p\text{CO}_2$ (1200 μatm), hypoxia (4.0 mg/L) and combined high $p\text{CO}_2$ /hypoxia. I also measured the activities of key metabolic enzymes (citrate synthase and lactate dehydrogenase) under combined high $p\text{CO}_2$ /hypoxia to assess the stressors' effects at the biochemical level. I found that gene expression patterns over time varied significantly among the three treatments, with little functional overlap among genes responsive to each treatment. In response to elevated $p\text{CO}_2$, blue rockfish increased expression of genes encoding muscular contractile proteins as well as genes involved in ATP metabolism pathways, possibly indicating shifts in muscle composition and heightened basal metabolism. Under hypoxia, blue rockfish also up-regulated genes encoding ATP metabolic proteins, but also up-regulated important ionoregulatory proteins like carbonic anhydrase. Under combined high $p\text{CO}_2$ and hypoxia, I observed differential expression of genes involved in various signaling pathways and oxygen carrying capacity, but observed no changes in metabolic enzyme activities. While blue rockfish up-regulated many of the same genes under combined high $p\text{CO}_2$ /hypoxia that were observed under each independent stressor, the response under both stressors was not additive but varied with exposure time between synergism and antagonism. My findings indicate that juvenile blue rockfish may be equipped to cope with moderate high $p\text{CO}_2$ and hypoxia in the short term, and that the species may be sufficiently responsive to employ different gene suites under each stressor. If rockfishes in general display tolerance to these stressors, annual recruitment may continue to play a larger role in determining abundances than climate-related oceanographic shifts. If changing conditions are shown to adversely impact some rockfish species more than others, however, environmental forecasting data may merit inclusion in California groundfish fishery management.

TABLE OF CONTENTS

	PAGE
ABSTRACT	iv
LIST OF TABLES	vi
LIST OF FIGURES	vii
ACKNOWLEDGEMENTS	viii
SECTION	
1 INTRODUCTION	1
Marine Stressors: Ocean Acidification and Hypoxia.....	1
Responses of Fish to Ocean Acidification and Hypoxia	2
Study Species: Blue Rockfish.....	5
RNA Sequencing	6
Research Questions and Hypotheses	7
2 METHODS	10
Fish Collection, Husbandry and Seawater Chemistry	10
RNA Extraction, cDNA Library Preparation and Sequencing	11
De Novo Transcriptome Assembly.....	13
Differential Gene Expression Analysis.....	14
Metabolic Enzyme Activity Assays.....	15
3 RESULTS	17
Fish Husbandry and Seawater Chemistry	17
RNA Extraction, cDNA Library Preparation and Sequencing	17
De Novo Transcriptome Assembly.....	18
Differential Gene Expression Analysis.....	18
Metabolic Enzyme Activity Assays.....	28
4 DISCUSSION.....	31
REFERENCES	38
A APPENDIX A: SUPPLEMENTARY TABLES	50

LIST OF TABLES

	PAGE
Table S1. Weights, standard lengths and total lengths for all blue rockfish individuals.....	50
Table S2. Mean carbonate chemistry conditions in the experimental system	52
Table S3. Blue rockfish tissue samples used for <i>de novo</i> transcriptome construction	52
Table S4. Sequencing information for all single-end and paired-end cDNA libraries.....	53
Table S5. UniProtKB IDs for differentially expressed blue rockfish muscle genes	55

LIST OF FIGURES

	PAGE
Figure 1. Experimental design of the acute high $p\text{CO}_2$ /hypoxia time-course.....	11
Figure 2. Differential gene expression totals over time versus the control treatment	19
Figure 3. Heatmaps depicting gene expression patterns over time in each treatment	21
Figure 4. PANTHER gene ontology pathways present in experimental treatments.....	25
Figure 5. Genes up- and down-regulated in experimental treatments and overlap	27
Figure 6. Boxplots depicting LDH enzyme activity over time in muscle, gill and liver	29
Figure 7. Boxplots depicting CS enzyme activity over time in muscle, gill and liver	30

ACKNOWLEDGEMENTS

I gratefully thank Dr. Cheryl Logan, Dr. Nathaniel Jue and Dr. Scott Hamilton for their presence on my thesis committee and valuable guidance. I also thank Jacob Green, Annette Verga-Lagier, Melissa Meredith, David Deering, Wenda Ly, Sasha Wheeler, Kirsten Boyer, Jacoby Baker, Kristin Saksa, Melissa Palmisciano and the many undergraduate and graduate students who assisted with this research. Additionally, I thank Dr. Kristy Kroeker, Sarah Lummis and Emily Donham for their assistance with seawater carbonate chemistry analysis. Lastly, I thank Neosha Kashef and Dave Stafford for their supervision during fish husbandry.

This work was funded by the National Science Foundation (NSF award EF-1416895 to Dr. Cheryl Logan of CSU Monterey Bay and award EF-1416919 to Dr. Scott Hamilton of Moss Landing Marine Laboratories and Dr. Susan Sogard of the NOAA Southwest Fisheries Science Center). Additional funding sources were the California State University Council on Ocean Affairs, Science and Technology (COAST), the Dr. Earl H. and Ethel M. Myers Oceanographic Trust, and the California State University Program for Education and Research in Biotechnology (CSUPERB). This work also used the Vincent J. Coates Genomics Sequencing Laboratory at UC Berkeley, supported by the National Institutes of Health (NIH) S10 OD018174 Instrumentation Grant.

SECTION 1

INTRODUCTION

MARINE STRESSORS: OCEAN ACIDIFICATION AND HYPOXIA

Shifting marine chemistry associated with global climate change such as ocean acidification (OA) and hypoxia will have both predictable and unanticipated effects on marine organisms (Fabry *et al.* 2008, Kroeker *et al.* 2010, Hoegh-Guldberg and Bruno 2010). Approximately 30-50% of atmospheric CO₂ has dissolved into the ocean, leading to decreases in ocean surface pH (Sabine *et al.* 2004, Orr *et al.* 2005). Mean surface pH levels have fallen by approximately 0.11 pH units since the Industrial Revolution, corresponding to a 30% increase in pH (IPCC, 2014). Separately, marine deoxygenation is projected to increase as climate change progresses (Breitburg *et al.* 2018). Oxygen solubility declines as water temperature increase, and increased stratification reduces mixing of oxygenated upper layers and deeper oxygen-poor layers (Meire *et al.* 2013). Extreme low oxygen and anoxia have already been observed in the California Current Large Marine Ecosystem (CCLME), driven by stratification and upwelling of hypoxic water onto the continental shelf (Bograd *et al.* 2008, Chan *et al.* 2008).

In the CCLME, northerly spring winds in April-August move surface waters offshore that are replaced by cold, nutrient-rich, acidic, hypoxic water from greater depths in a phenomenon known as upwelling (Feely *et al.* 2008). Climate change is projected to alter the frequency, intensity and duration of these coastal upwelling events (Bakun 1990, Snyder *et al.* 2003, Bakun *et al.* 2015, Brady *et al.* 2017). Typically, upwelled waters intrude into nearshore ecosystems on the scale of hours to days as strong, but intermittent alongshore winds drive surface waters offshore (Booth *et al.* 2012). These short-term events may become more prolonged and more frequent, however, as northerly winds are strengthened by increasing pressure gradients between land and sea (Sydemann *et al.* 2014). Even if upwelling patterns remain unchanged, upwelled waters in the CCLME will likely see continued climate-driven decreases in background DO and pH (Bograd *et al.* 2008, Booth *et al.* 2012), due to global CO₂

emissions. These forecasts raise questions about the ability of nearshore organisms such as teleost fishes to effectively cope with high $p\text{CO}_2$ and hypoxia during longer and more severe events. Understanding the responses of teleosts to these stressors has been identified as a priority by biologists, fishermen, policymakers, and consumers of marine products (Costanza *et al.* 1997, Hoegh-Gulberg and Bruno 2010, Cheung *et al.* 2010, Natl. Res. Council 2010, Natl. Res. Council 2011).

RESPONSES OF FISH TO OCEAN ACIDIFICATION AND HYPOXIA

Although most teleosts are known to effectively buffer against internal pH changes via bicarbonate retention and other strategies (Cameron 1978, Cameron and Iwama 1989), negative effects on behavior, growth, development, survival, metabolic rate and swimming performance have now been reported in many species (reviewed in Heuer and Grosell 2014). Traits impacted by OA include decreased growth in juvenile Atlantic cod (Moran and Støttrup 2011), disturbances in homeostatic pH regulation in bream (Michaelidis *et al.* 2007) and depressed metabolic rates, aerobic scope and cardiorespiratory function in other species (Gilmour 2001, Munday *et al.* 2009a, Enzor *et al.* 2013, Gilmour 2007). Behaviorally, reef fishes have been shown to be adversely impacted in their olfactory and auditory capabilities, suggesting that early life stages may be vulnerable if their changed behavior exposes them to increased predation or reduces their settlement success (Munday *et al.* 2009b, Munday *et al.* 2010, Simpson *et al.* 2011). Molecularly, these changes appear to be driven by altered cell membrane ion gradients impacting the function of the GABA neurotransmitter and its GABA_A receptors (Nilsson *et al.* 2012). After chronic OA exposure, some studies report up-regulation of transcripts encoding important ion-exchanger proteins like the Na^+/K^+ ATPase pump (NKA), AE1, NBC1, NHE2, NHE3 transporters and carbonic anhydrase (Deigweiher *et al.* 2008, Tseng *et al.* 2013). Additionally, numerous metabolic processes are apparently reduced in fish by combined warming and high $p\text{CO}_2$, including mitochondrial respiration and both aerobic and anaerobic (glycolytic) enzyme activities (Strobel *et al.* 2012, Strobel *et al.* 2013a, Strobel *et al.* 2013b). Interestingly, some studies have reported partial compensation for these metabolic shifts in certain tissues like red muscle and liver

(Strobel *et al.* 2013a, Strobel *et al.* 2013b). It must also be noted that some studies on teleosts have observed no change (Maneja *et al.* 2013, Jutfelt and Hedgärde 2013, Hamilton *et al.* 2017) or even improvements in physiological performance under OA (Melzner *et al.* 2009, Miller *et al.* 2013).

Hypoxia is a separate marine stressor that is often coincident with low pH (Melzner *et al.* 2013). To cope with low levels of dissolved oxygen (DO), fishes must employ mechanisms to increase oxygen supply or decrease demand (Richards 2009, Claireux and Chabot 2016). Short-term responses to increase oxygen supply include elevated ventilation rates to increase flow of water over the gills (Randall 1982), increased erythrocyte counts and/or hemoglobin affinity for oxygen in blood (Randall 1982, Val 1995) and increases in gill lamellae surface area (Randall 1982, Wu and Woo 1985). If aerobic metabolism is impacted by a lack of oxygen, some fish will increase reliance on anaerobic metabolic pathways (Goolish 1991). Under severe hypoxia, oxygen demand can be decreased through metabolic suppression (Wu 2002). At the molecular level, hypoxia-inducible factors (HIFs) have been shown to control transcription of genes involved in the hypoxic response such as growth factors, metabolic enzymes and erythropoietin (Wu 2002). In eukaryotes, some HIFs have been identified as master initiators of a complicated signaling cascade, while prolyl hydroxylases (PHDs) have been suggested as additional regulators in teleosts (Gracey *et al.* 2001, Terova *et al.* 2008, Xiao *et al.* 2015). Additionally, metabolic depression and shifts towards anaerobiosis are often accompanied by signs of a cellular stress response (CSR), down-regulation of protein synthesis, post-transcriptional and post-translational modifications, inhibition of growth processes, and reduction in adenosine trisphosphate (ATP) production and turnover (Gracey *et al.* 2001, Wu 2002, Terova *et al.* 2008).

Research on the interaction of OA and hypoxia in teleosts is presently minimal, but highly relevant in upwelling systems. Responses to individual stressors may interact additively, antagonistically or synergistically (Kroeker *et al.* 2013). For example, increased ventilation to sustain oxygen uptake may subject fish to internal hypercapnia (elevated CO₂ in fluids/tissues) and acidosis (increased acidity/lower pH of fluids) as more CO₂ diffuses across gill epithelia (Heuer and Grosell 2014, Miller *et al.* 2016). A recent study in juvenile summer flounder (*Paralichthys dentatus*) examined the effects of

diel cycling of moderate and extreme, independent and combined DO and pH over a period of 20 days (Davidson *et al.* 2016). Flounder experienced reductions in growth rate at the extreme low DO level across all pH levels, but there was no other evidence of changes in growth rate in any other independent or combined treatments, suggesting that growth was primarily hindered by hypoxia rather than hypercapnia. A study of the combined-stressor effects on two larval *Menidia* congeners and larval *Cyprinodon variegatus* suggested that even closely related species exhibit different responses (DePasquale *et al.* 2015). Survival of *M. beryllina* decreased under low pH (7.4) alone, while both survival and size of *M. beryllina* were influenced negatively and additively by low DO and low pH. Survival of *M. menidia* decreased synergistically under low DO and low pH, but survival of *C. variegatus* was not impacted by either the independent or combined stressors. The growing body of literature on these interactions indicates that, much like under independent hypoxia and OA (Vaquer-Sunyer and Duarte 2008, Heuer and Grosell 2014, Cattano *et al.* 2018), there is a broad range of sensitivities across taxa.

Predicting the effects of multiple climate drivers like high $p\text{CO}_2$ and hypoxia can be challenging (Crain *et al.* 2008, Kroeker *et al.* 2017). Recently, models of stressor interactions have been proposed that consider the direction of stressor effects (positive or negative) (Piggott *et al.* 2014, Côté *et al.* 2016). Responses may be classified as (i) additive; where the response to the combined treatment is equal to the sum of the responses to the individual stressors, (ii) synergistic; where the response is greater than the sum of the responses to the individual stressors, or (iii) antagonistic, where the response is less than the sum of the responses to the individual stressors. Antagonism can occur if similar pathways are used to respond to individual stressors, whereas synergistic responses can occur if one stressor inhibits the response pathway required to respond to a second stressor. Coupled OA and hypoxia have been shown to have negatively additive and synergistic effects on coastal organisms, and like the stressors independently, affect even closely related taxa differentially (Gobler *et al.* 2014, Gobler and Baumann 2016, Davidson *et al.* 2016).

In some fishes, insufficient compensation for low pH or hypoxia has been observed to induce a cellular stress response (CSR). CSR proteins can be involved in molecular chaperoning, ubiquitination, DNA damage repair, oxidative stress, immune

system functions, and apoptosis (Kültz 2005). The CSR in fish is most frequently documented in response to elevated temperature (Smith *et al.* 2013, Qian *et al.* 2014), but some studies report up-regulation of CSR heat-shock chaperones and DNA damage-inducible transcripts under OA (Dennis *et al.* 2015, Huth and Place 2016). In a study that examined acute and chronic gene expression under high $p\text{CO}_2$ and warming in an Antarctic notothenioid (*Trematomus bernacchii*), a significant CSR response was documented that tapered to near-basal levels after 50 days (Huth and Place 2016). Another recent study described increases in CSR gene suites after five months of exposure to $p\text{CO}_2$ levels above 1900 μatm in copper rockfish (*Sebastes caurinus*) and a similar CSR in blue rockfish (*S. mystinus*) that was induced at $p\text{CO}_2$ levels as low as 750 μatm (Hamilton *et al.* 2017). Separately, the CSR in fish under hypoxia has been documented primarily at extreme low oxygen levels (Fuzzen *et al.* 2011).

STUDY SPECIES: BLUE ROCKFISH

Sebastes (Teleostei: Sebastidae: *Sebastes*) congeners may exhibit differential responses to OA in their behavior, aerobic physiology, gene expression patterns, enzyme activities and overall metabolic poise (Hamilton *et al.* 2017, Davis *et al.* 2018). Varying behavioral patterns, depth distributions, habitat requirements, larval durations, and settlement behavior have been observed among *Sebastes* and may contribute to their divergent tolerances (Love *et al.* 1990, Leaman 1991). As juveniles, for example, copper rockfish recruit from the open ocean after a 1-2 month pelagic larval duration (PLD) to nearshore kelp forest canopies. Blue rockfish juveniles also settle in kelp forests, but recruit closer to the benthos after a 3-4 month PLD (Lenarz *et al.* 1991, Love *et al.* 2002). It has been suggested that because benthic and upwelled seawater tend to be colder, more acidic and more hypoxic compared with surface waters in kelp forests, juvenile blue rockfish may have acclimatized or adapted to these conditions (Frieder *et al.* 2012, Hamilton *et al.* 2017, Koweeck *et al.* 2018). Furthermore, gravid adult blue rockfish typically undergo parturition during winter months, allowing the young-of-year to develop more before the onset of spring upwelling than species that give birth during the spring, like copper rockfish. Blue rockfish are of interest to both biologists and managers

due to their abundance in Californian waters and their significance to the state's recreational and commercial groundfish fishery (Key *et al.* 2008, Dick *et al.* 2017).

RNA SEQUENCING

The utility of next-generation sequencing (NGS) techniques in ecological studies is increasing as their costs continue to fall (Ekblom and Galindo 2011, Todd *et al.* 2016). Initially developed for biomedical purposes, NGS allows millions of copies of an organism's genes to be sequenced from a minimal amount of starting material. Using fluorescent dyes and ligands, specialized polymerase enzymes and advanced spectrophotometric techniques, the specific nucleotides of the deoxyribonucleic acid (DNA) molecules that comprise genes can be determined. Cloud, cluster and server computing have emerged as platforms powerful enough to analyze the massive datasets produced by NGS. More recently, sequencing of complementary DNA (cDNA) produced from ribonucleic acid (RNA) has also become feasible. Messenger RNA (mRNA) is the molecule produced by transcription of DNA coding regions and often contains alternatively spliced gene exons and other interesting expression information. mRNA's role as a "middleman" between information-coding DNA and the functional proteins that make up a phenotype has distinguished the transcriptome, or the global expression of mRNA molecules in a tissue or organism, as a valuable source of information on species' molecular physiology (Wang *et al.* 2009). Quantifying temporal transcriptional regulation in tissues can provide insight into the different types and quantities of proteins that species must produce in response to dynamic environmental conditions (Garcia *et al.* 2012, Qian *et al.* 2014, Long *et al.* 2015, Oomen and Hutchings 2017). One important consideration in interpreting transcriptomic data, however, is that mRNA expression does not always correlate with nor account for cumulative protein expression (Liu *et al.* 2016). For example, some genes are not transcriptionally regulated or are modified post-transcription or post-translation (Schwanhausser *et al.* 2011).

Despite some biological limitations, RNA sequencing can now determine the relative abundances of thousands of RNA transcripts in a given cell or tissue. This process and the associated techniques are now known collectively as RNA-seq. Perhaps

the greatest advantage of RNA-seq is that it does not require a complete genome to estimate gene expression. The transcriptome to which reads are mapped is generally much smaller and simpler to construct than a genome (Grabherr *et al.* 2011). Moreover, the unbiased nature of RNA-seq fosters hypothesis generation and the discovery of novel transcripts and expression patterns not explicitly predicted by the researcher *a priori*. These facts distinguish RNA-seq as well-suited for examination of DGE in non-model species.

RNA-seq has been used to identify differential gene expression (DGE) patterns across non-model fish species under different stressors (Palstra *et al.* 2013, Smith *et al.* 2013, Qian *et al.* 2014, Logan and Buckley 2015, Huth and Place 2016, Hamilton *et al.* 2017). Such work has helped identify molecular pathways, physiological responses and biomarker genes that describe the mechanisms underlying the condition of ecologically and economically important species. Combining high-throughput transcriptomic data with examination of other sub-organismal responses to environmental stressors represents an integrative approach to uncovering the mechanistic underpinnings of changes in teleost physiology (Komoroske *et al.* 2015, Hamilton *et al.* 2017).

RESEARCH QUESTIONS AND HYPOTHESES

To date, the responses of blue rockfish to independent and combined high $p\text{CO}_2$ and hypoxia over short timescales emulating the duration of an upwelling event have not been investigated. A recent comprehensive study, however, has provided an intriguing comparison of juvenile blue and copper rockfish responses after chronic exposure to high $p\text{CO}_2$ at behavioral, physiological and molecular levels (Hamilton *et al.* 2017). The data presented in this study suggest that in response to OA, blue rockfish are better able to retain their overall aerobic performance, induce greater changes in gene expression, and are less affected in the activities of key metabolic enzymes than copper rockfish. To determine whether or not these responses hold true during the initial days to weeks over which upwelling events typically occur, and to examine the interaction of high $p\text{CO}_2$ and hypoxia, we sought to answer three questions: 1) How do juvenile blue rockfish alter gene expression in their white muscle tissue in response to short-term independent and

combined high $p\text{CO}_2$ and hypoxia? 2) Do juvenile blue rockfish exhibit an additive, synergistic or antagonistic response to combined high $p\text{CO}_2$ and hypoxia in terms of both the number and function of differentially expressed genes? 3) Do blue rockfish increase anaerobic metabolism in their white muscle, gills and liver in response to short-term combined high $p\text{CO}_2$ and hypoxia (as measured by enzyme activities of citrate synthase, an aerobic indicator, and lactate dehydrogenase, an anaerobic indicator)?

To answer these questions, we exposed juvenile blue rockfish to independent high $p\text{CO}_2$, independent hypoxia, combined high $p\text{CO}_2$ and hypoxia, and a control treatment for two weeks and sampled dorsal white muscle, gill and liver tissues at 12 h, 24 h and two weeks of exposure to examine the effects of acute and prolonged upwelling. We performed RNA-seq on white muscle, which comprises a large portion of fish biomass (white muscle RNA-seq data are also directly comparable to data generated from the same tissue in previous studies). We also performed targeted enzyme activity assays on white muscle, gill and liver, tissues in which sub-organismal metabolic shifts may be observed.

Per RNA-seq, we hypothesized that juvenile blue rockfish would respond to high $p\text{CO}_2$, hypoxia and the combined stressors through differential expression of tens to hundreds of genes as compared with control fish, although fewer or greater numbers of genes could be differentially expressed if the stressor effects were lesser or greater than anticipated. Under the combined stressors, we anticipated either an additive response in which the rockfishes' responses to independent high $p\text{CO}_2$ and hypoxia were present under the combined stressors, or a synergism in which the responses interacted and stimulated novel responses like a sustained CSR. Given the findings of previous studies, we anticipated that classic signs of mild cellular stress like molecular chaperones (i.e. heat-shock proteins or HSPs), oxidative stress, increased transcription, DNA damage and ubiquitination would be up-regulated at the 12 h and 24 h timepoints in the high $p\text{CO}_2$, hypoxia and combined high $p\text{CO}_2$ /hypoxia experimental treatments. At two weeks of exposure, we expected that these gene expression signatures would taper to levels approximating those observed after five months (Hamilton *et al.* 2017). At the two-week timepoint in the experimental conditions, we anticipated up-regulation of genes involved in more chronic responses like muscular restructuring. In the hypoxic and combined

stressor treatments, we expected signs of increased oxygen transport and transcriptional regulation in the form of transcription factors. Up-regulation of energetically intensive processes that would increase oxygen supply, like angiogenesis and erythropoiesis, were also expected. Quantitatively, we anticipated that the combined stressors would induce an additive or synergistic response (i.e. the number of genes differentially expressed under both stressors would be equal to or greater than the sum of the genes expressed under each individual stressor). Qualitatively, an additive response under the combined stressors would include functional gene categories present under both the individual stressors, while a synergistic response would include additional categories such as a CSR or metabolic processes that were not utilized under either of the independent stressors (Piggott *et al.* 2015, Côté *et al.* 2016).

In terms of metabolic enzyme activity, we hypothesized that juvenile blue rockfish would exhibit increased anaerobic metabolism relative to aerobic metabolism (i.e. increased LDH:CS ratios) during exposure to combined high $p\text{CO}_2$ /hypoxia as compared with control fish. We expected that these changes would be driven by increases in LDH activity and/or decreases in CS activity. Prior studies report that critical swimming speed, aerobic scope and LDH:CS ratios were not affected in blue rockfish after chronic exposure (five months) to extreme high $p\text{CO}_2$ (Hamilton *et al.* 2017). We expected that the shift towards anaerobic metabolism would be greatest at 12 h and subsequently taper to lower LDH:CS ratios that still remained significantly elevated above those observed in control fish. To our knowledge, this is the first study to examine the individual and combined effects of high $p\text{CO}_2$ and hypoxia on gene expression and enzyme activity in teleosts.

SECTION 2

METHODS

FISH COLLECTION, HUSBANDRY AND SEAWATER CHEMISTRY

In June 2016, we collected 80 juvenile blue rockfish recruits near the benthos of the kelp forest and rocky reef environment of Stillwater Cove in Carmel, California on SCUBA using hand nets. Blue rockfish morphology and life history are similar to those of a recently identified cryptic species, the deacon rockfish (*S. diaconus*; Frable *et al.* 2015), but deacon rockfish are more common at higher latitudes north of the Monterey Bay. Thus, no effort was made to distinguish the possibility that both species were collected.

Rockfishes were transported in 12° C seawater to Moss Landing Marine Laboratories in Moss Landing, CA and held in ambient flow-through seawater (FSW) for one month for lab acclimation. During acclimation, fish were fed thawed krill *ad libitum* every 48 hours. All fish were then transported in 12° C seawater to the NOAA Southwest Fisheries Science Center in Santa Cruz, CA for the experiment. Juveniles were placed in 100 L black cylindrical aquaria with plastic mesh serving as simulated habitat and acclimated in ambient FSW for one week, after which we immediately placed 20 individuals in each of four seawater treatments for two weeks: ambient ($p\text{CO}_2 \sim 400 \mu\text{atm}$, $\text{pH} \sim 8.0$, $\text{DO} \sim 8 \text{ mg/L}$), high $p\text{CO}_2$ /low pH ($p\text{CO}_2 \sim 1200 \mu\text{atm}$, $\text{pH} \sim 7.6$, $\text{DO} \sim 8 \text{ mg/L}$), low DO ($p\text{CO}_2 \sim 400 \mu\text{atm}$, $\text{pH} \sim 8.0$, $\text{DO} \sim 4 \text{ mg/L}$), and a “combined” treatment at both high $p\text{CO}_2$ and low DO levels ($p\text{CO}_2 \sim 1200 \mu\text{atm}$, $\text{pH} \sim 7.6$, $\text{DO} \sim 4 \text{ mg/L}$). Control fish were removed and placed back into ambient conditions to control for handling stress. Temperature was maintained across all treatments using a system of chillers, ranging from 11.4-12.3° C due to natural fluctuations in incoming seawater. Fishes were fed thawed krill *ad libitum* every 48 h, with at least a 48 h starvation period prior to each experimental time-point to avoid gene expression changes associated with specific dynamic action. We quickly weighed the fish and measured their standard and total lengths (Table S1) before dissecting them and flash-freezing white muscle, gill and liver

tissues from $n=4$ individuals from each treatment at three time-points: 12 h, 24 h and two weeks (Figure 1). The Institutional Animal Care and Use Committee (IACUC) at San Jose State University approved this research on protocol #1007. Scientific collecting to hold fish in captivity was permitted by the California Department of Fish and Wildlife on permit #SC-6477.

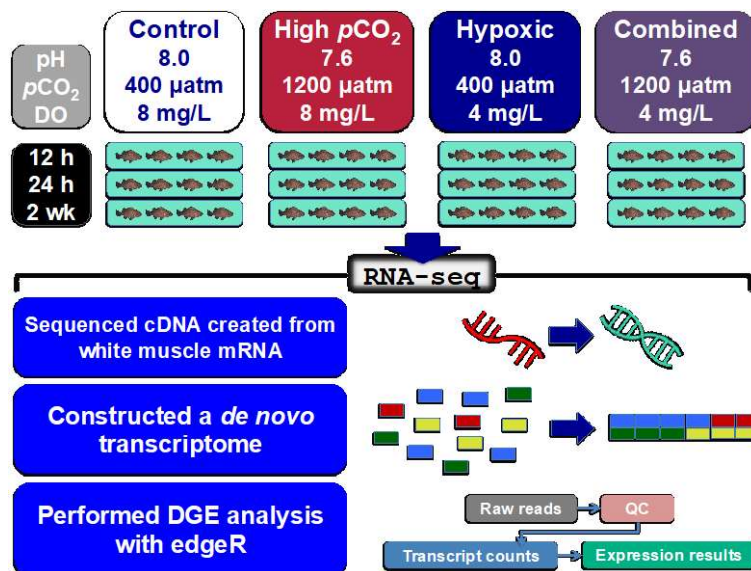


Figure 1. Experimental design of the acute high $p\text{CO}_2$ /low DO time-course in which blue rockfish were exposed to four seawater treatments and RNA-seq was performed on their dorsal white muscle tissue.

$p\text{CO}_2$ and DO levels were maintained at the treatment set points by bubbling CO_2 and N_2 gas, respectively, into intermediary 500 L reservoirs with recirculation pumps, each feeding two replicate treatment tanks (Table S2). Gas flow was controlled via solenoid valves and regulated by Loligo[®] Systems CapCTRL[™] and WitroxCTRL[™] software. Temperature, pH and DO were checked daily in all tanks with a Hach[®] HQ40D[™] portable multi-meter and pH values were corrected using Tris buffer pH measurements at temperature. We collected water samples at zero hours, one week and two weeks in accordance with best practices and assessed total alkalinity using a Metrohm[®] 855[™] robotic titrosampler (Riebesell *et al.* 2010). pH was measured using *m*-cresol dye in a spectrophotometer at 440, 560, and 730 nm (Dickson *et al.* 2007). Carbonate chemistry parameters were calculated using CO2SYS version 1.0.3 (Pierrot *et al.* 2006).

RNA SEQUENCING, cDNA LIBRARY PREPARATION AND SEQUENCING

We extracted total RNA from a total of 48 white muscle tissue samples ($n=4$ fish per treatment per time point) using an RNeasy Plus Mini™ Kit (Qiagen®, Valencia, CA; cat. no. 74134). Briefly, we homogenized 15-30 mg of tissue from each sample in RLT lysis buffer with a 5 mm stainless steel bead using a Qiagen® TissueLyser LT™ at 50 Hz for three minutes. Genomic DNA (gDNA) was removed with a spin column. Total RNA was eluted into 50 μ L of nuclease-free water and quantified using a NanoDrop™ 2000 spectrophotometer and a Qubit® 2.0 fluorometer (Qubit® RNA Broad Range Assay kit, Invitrogen™, cat. no. Q10210). RNA integrity was assessed and RNA Quality Numbers (RQNs) were calculated using an Advanced Analytical® Fragment Analyzer™ (High Sensitivity RNA Analysis Kit, Advanced Analytical®, cat. no. DNF-472-0500). One microgram of high quality total RNA (RQN > 8.0) from each blue rockfish muscle tissue sample was used to prepare complementary DNA (cDNA) libraries.

We isolated mRNA and constructed 48 cDNA libraries using two Illumina® TruSeq™ Stranded mRNA Library Preparation Kits (Illumina®, cat. no. RS-122-2101 and RS-122-2102, Adaptor Sets A and B) (Figure 1). Libraries were prepared in two sets of 24 and randomized to account for batch effects. Briefly, we removed ribosomal and other non-coding RNAs to purify messenger RNA (mRNA) and fragmented the isolated mRNA. We synthesized first strand cDNA using SuperScript III Reverse Transcriptase (Invitrogen™, cat. no. 18080-044), and second strand cDNA using the 2'-deoxyuridine 5'-triphosphate (dUTP) nucleotide method for strand specificity. We then ligated a unique adapter index to each cDNA library and amplified the libraries through 15 cycles of polymerase chain reaction (PCR). cDNA purification steps were completed with PCRClean™ DX paramagnetic beads (Aline Biosciences®, cat. no. C-1003-5) and Agencourt AMPure™ XP beads (Beckman-Coulter®, cat. no. A63881). We quantified cDNA concentrations using a Qubit® 2.0 fluorometer and Qubit® dsDNA High Sensitivity Assay kit (Invitrogen™, cat. no. Q32851) and verified that fragments were distributed in the 260-320 bp range using an Advanced Analytical® Fragment Analyzer™ (High Sensitivity Large Fragment Analysis Kit, Advanced Analytical®, cat. no. DNF-493-0500). Adapter dimers were removed with a 1.2X bead:sample volume

clean-up step. Libraries were randomly multiplexed and sequenced in equal numbers in each of two 50 base-pair (bp) single-end (SE) lanes on a HiSeq4000 platform at the Vincent J. Coates Genomics Sequencing Laboratory (GSL) at the University of California, Berkeley.

DE NOVO TRANSCRIPTOME ASSEMBLY

To create a *de novo* blue rockfish reference transcriptome, we prepared cDNA libraries from eight additional blue rockfish brain, liver, gill and muscle tissue samples harvested after various low pH and hypoxia exposures using the procedure described in *RNA Sequencing, cDNA Library Preparation and Sequencing* (Table S3). The one exception to this procedure was that these eight libraries were multiplexed and sequenced in one 150 base-pair paired-end (PE) HiSeq4000 sequencing lane at GSL; longer reads were used to improve the quality of the *de novo* assembly.

We used FastQC to assess the quality of the raw sequence reads in both the SE (time-course) and PE (*de novo*) cDNA libraries (Andrews 2010). For all pass-filter reads in the SE libraries, we used Trimmomatic to remove adapter sequences, trim the reads base-by-base for quality (Phred quality scores > 5 retained) and discard short reads (< 25 bp in length) after trimming (Bolger et al. 2014, MacManes 2014). We then performed FastQC again on the QC-processed data (Table S4).

Using Trinity software (v2.3.2, Haas *et al.* 2013), we built a *de novo* transcriptome assembly for blue rockfish using the eight libraries from the PE sequencing lane along with three additional SE libraries from the experimental time-course that ensured representation of genes expressed during the exposure (indicated by asterisks *, Table S3). The sequence file type was fastq, the maximum memory allocated was 50 GB, the strand-specific library type was specified as reverse-forward (RF) per the dUTP method of ensuring strand specificity, and 20 central processing units (CPUs) were allocated to perform the assembly. We used default Trimmomatic quality trimming parameters to trim the raw reads as well as the *in silico* digital read normalization argument to remove excess reads and reduce computing time. Assembly quality was

assessed using the Trinity program Trinity.Stats.pl to determine the number of contigs and N_x statistics.

We annotated the full assembly against the UniProtKB and NCBI non-redundant (nr) *Actinopterygii* protein databases using DIAMOND (Buchfink *et al.* 2015). We identified putative gene functions using a single, broad level of gene ontology (GO) pathways by entering UniProtKB identifiers into the PANTHER classification system (www.pantherdb.org, Mi *et al.* 2019a, Mi *et al.* 2019b). To assess the biological completeness of the assembly, we used the Actinopterygii (ray-finned fishes) database of Benchmarking Universal Single-Copy Orthologs (BUSCOs) to assess the biological completeness of the assembly by verifying the presence of conserved orthologs (Simão *et al.* 2015).

DIFFERENTIAL GENE EXPRESSION ANALYSIS

We used the same quality control procedures and parameters on the SE blue rockfish sequences as on the PE sequences used to create the *de novo* assembly. After filtering and trimming reads from the SE cDNA libraries, we mapped the reads to the blue rockfish *de novo* assembly using Bowtie (Langmead *et al.* 2009) and estimated transcript abundance using RNA-Seq by Expectation-Maximization (RSEM) (Li and Dewey 2011). We produced transcript abundance matrices and performed differential gene expression (DGE) analyses with a false discovery rate (FDR)-corrected q-value threshold of 0.05 with no fold change requirement using the Bioconductor package edgeR (Robinson *et al.* 2010).

To compare the effects of each individual stressor and the combined stressors on gene expression, we performed a separate DGE analysis at each time-point of interest (12 h, 24 h and two weeks) and a separate DGE analysis for each of the four treatments across time for a total of seven analyses. This design allowed for a detailed analysis of the fishes' responses at each time-point as well as a comparison of total DGE levels over time. edgeR calculates differential expression of a given gene relative to the mean expression level of that gene across all samples used in the analysis. We created heatmaps in the R programming environment using the “ggplot2” package, grouping

columns by treatment and rows (genes) by hierarchical clustering. We identified putative gene functions through gene ontology (GO) categories by entering UniProtKB identifiers into PANTHER and manually reviewing relevant literature. To test for over-representation of GO categories in DGE lists from each of the three experimental treatments, we performed the built-in PANTHER statistical over-representation test on each of the three lists of UniProtKB identifiers (test type: Fisher's Exact; correction: false discovery rate).

To examine interaction effects between the two individual stressors and the combined treatment, we used total numbers of DE genes and GO categories observed in each treatment without assigning directionality (i.e. "positive" or "negative") to the responses. Responses to high $p\text{CO}_2$ and hypoxia combined treatment were first classified as additive, synergistic or antagonistic based on numbers of differentially expressed genes (i.e., additive if number DE genes in the combined treatment were nearly equal to the sum of the responses to the individual stressors; synergistic if there were more genes responsive than the sum, or antagonistic if there were fewer genes). Next, we examined the PANTHER pathway categories for signs of functional overlap in genes responsive to the individual and combined treatments.

METABOLIC ENZYME ACTIVITY ASSAYS

We also tested for shifts towards anaerobic metabolism by measuring enzymatic activity of citrate synthase (CS) and lactate dehydrogenase (LDH) in muscle, gill and liver of rockfishes from the control and combined high $p\text{CO}_2$ /hypoxia treatments at 12 h, 24 h and two weeks. These enzymes are established indicators of aerobic and anaerobic (glycolytic) metabolism in fishes, respectively (Childress and Somero 1990). We assayed CS and LDH activities at 30° C on a Tecan Infinite[®] M200 Pro[™] microplate reader, using a previously described protocol with slight modifications (Hamilton *et al.* 2017). Briefly, we homogenized 5-30 mg of frozen tissue at a 1:10 tissue:buffer dilution for four minutes at 50 Hz in ice-cold monobasic/dibasic potassium phosphate (K_2HPO_4) buffer (pH 6.8 at 20° C) (tissue masses varied between 5-30 mg due to differences in the average mass of each tissue type that was successfully dissected and preserved). Homogenates

were centrifuged twice at 13,000 x g for 10 minutes and serially diluted to working concentrations. For CS assays, we diluted the tissue at a ratio of 1:50 tissue:buffer for all three tissues. For LDH assays, tissues were diluted to 1:1000 for white muscle, 1:500 for gill tissue, and 1:50 for liver due to large differences in activity between tissue types. These dilutions yielded the most linear and stable enzymatic reactions for each tissue type. We corrected for each tissue-specific dilution factor when normalizing activities to grams fresh weight of tissue (GFW) and grams fresh weight of protein (GFP).

The synthesis of citrate from acetyl coenzyme A and oxaloacetate was indirectly determined by the dethionation of 5,5-dithio-bis-[2-nitrobenzoic acid] (DTNB) and the appearance of TNB at 412 nm, while LDH activity was determined by the coupled oxidation of β -nicotinamide adenine dinucleotide (NADH) at 340 nm during reduction of pyruvate to lactate. Reaction absorbances were measured for 10 minutes, but only data collected between 2-5 minutes were used for the final analysis because this region yielded the greatest overall linearity and lowest variability between technical replicates across all tissue samples. Total protein content was determined using bicinchoninic acid (BCA) assays on a microplate reader (Pierce™ BCA Protein Assay, Thermo Scientific™, cat. no. 23225). Enzyme activities were calculated in International Units (IU) and normalized to GFW and GFP. We tested the six data sets (LDH and CS activities in muscle, gill and liver) for normality using Shapiro-Wilk tests ($p < 0.05$) and for homogeneity of variance using Levene's tests ($p < 0.05$). For any non-normal data sets, Box-Cox transformations were applied using the optimal Box-Cox transformation parameter (λ) as calculated in the "forecast" package in the R programming environment. Significant differences in enzyme activity across treatments and time were determined using a two-way Analysis of Variance (ANOVA) and Tukey *post hoc* tests.

SECTION 3

RESULTS

FISH HUSBANDRY AND SEAWATER CHEMISTRY

No mortality was observed in blue rockfish over two weeks under control conditions, high $p\text{CO}_2$, hypoxia, or the combined stressors. The average fish weight at the time of dissection was 1.62 ± 0.47 (SD) g and the average total length was 54.9 ± 3.5 (SD) mm (see Table S1). No effects of treatment or exposure time were observed on rockfish weights or total lengths (two-way ANOVA; $p > 0.05$). Temperature, $p\text{CO}_2$ and DO levels were maintained at the target set-points for the duration of the experiment (Table S2).

RNA EXTRACTION, cDNA LIBRARY PREPARATION AND SEQUENCING

We successfully extracted high-quality total RNA from 46 of 48 blue rockfish white muscle samples and synthesized high-yield cDNA libraries for 44 of 46 total RNA samples. Two cDNA libraries returned yields below the minimum requirement and were not sequenced. Fragment analysis of all sequenced libraries revealed primary cDNA peaks between 242-346 base-pairs. The trimmed SE reads used for differential gene expression analysis averaged 17,526,508 reads per library (min: 10,257,254; max: 35,798,493). The SE read mapping rate to the assembly ranged from 95.63-96.86% of all reads (unique and multi-mapped). Sequencing quality and quantity information is presented in Table S4. The data discussed herein have been deposited in NCBI's Gene Expression Omnibus (Edgar et al. 2002) and are accessible through GEO Series accession number **GSE129003**.

DE NOVO TRANSCRIPTOME ASSEMBLY

Eight high quality cDNA libraries were created for blue rockfish brain, liver, gill and muscle tissues from individuals held under control conditions, high $p\text{CO}_2$, low DO or the combined treatment (SRA accession nos. **SRR8717232**, **SRR8717233**, **SRR8717234**, **SRR8717235**, **SRR8717236**, **SRR8717237**, **SRR8717238**, **SRR8717239**). After Trimmomatic post-processing, 471,950,098 PE reads were retained with an average of 58,993,762 reads per library (min: 40,207,774; max: 84,764,890). The Trinity *de novo* reference transcriptome yielded 239,549 contigs (“genes”), 463,213 total transcripts (“isoforms”). The contig N_{50} value was 1,939 bp, with a median contig length of 420 bp and an average contig length of 948 bp. The assembly contained 94.7% of the Actinopterygii (ray-finned fishes) BUSCOs (34.0% single-copy orthologs; 60.7% duplicated orthologs). Using DIAMOND, we annotated 32.5% of the 463,213 unique transcripts assembled by Trinity to the UniProtKB/Swiss-Prot database (150,707 transcripts) and 43.3% to the Actinopterygii nr database (200,746 transcripts).

DIFFERENTIAL GENE EXPRESSION ANALYSIS

Bowtie mapping of high-quality reads retained after QC processing yielded a total mapping rate of 95.63-96.86% of all reads (unique and multi-mapped) to the newly produced blue rockfish *de novo* transcriptome assembly. Unique read mapping rates ranged from 57-61%. In the pairwise comparisons involving the control treatment across the three separate edgeR analyses performed at each time-point (i.e. control fish compared to treatment fish), we observed differential expression of 641 unique contigs (FDR<0.05). Of these, we successfully extracted UniProtKB accession codes and gene function information for 293 contigs (45.6%).

Gene expression profiles for the three experimental treatments were distinct over time, varying in both the types and quantities of DE transcripts. Our first analysis examined differential expression between the control and experimental treatments at each time-point separately. At 12 h, a total of 162 genes were differentially expressed across the three experimental treatments (FDR<0.05). At 24 h, 285 total genes were differentially expressed. After two weeks, 278 total genes exhibited differential

expression. Across all three time-points, 641 unique contigs were differentially expressed. Of these, we successfully extracted UniProtKB accessions for 293 contigs (45.7%, Table S5) and *nr* accessions for 394 contigs (61.3%).

Treatment effects over time: high $p\text{CO}_2$

Under elevated $p\text{CO}_2$, the number of overall DE genes (both up- and down-regulated) increased over time compared to the control treatment (Figure 2). After 12 h under high $p\text{CO}_2$, 24 genes were differentially expressed in blue rockfish muscle tissue (nine up-regulated, 15 down-regulated) compared to fish in the control treatment. At 24 h, 42 genes were differentially expressed (22 up-regulated, 20 down-regulated).

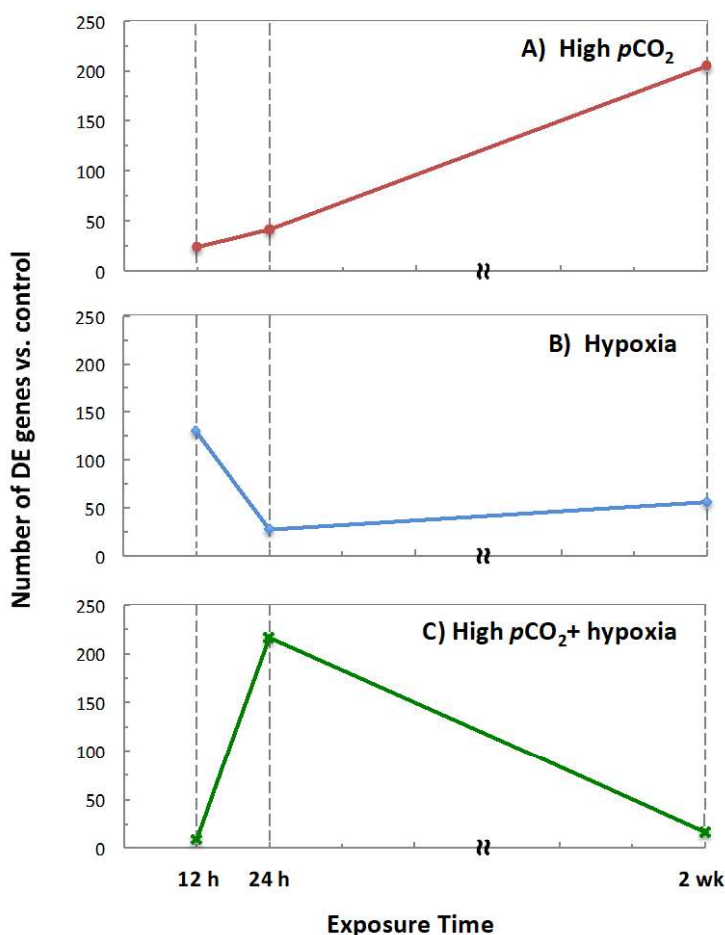


Figure 2: Total numbers of differentially expressed genes in blue rockfish white muscle under A) high $p\text{CO}_2$ B) hypoxia and C) high $p\text{CO}_2$ /hypoxia versus the control treatment (FDR<0.05).

After two weeks of exposure to high $p\text{CO}_2$, 205 genes exhibited differential expression, with the majority (146) displaying up-regulation (Figure 2).

At 12 h under high $p\text{CO}_2$, up-regulated genes included creatine kinase m-type (CKM), sarcoplasmic reticulum calcium ATPase 1 (SERCA1), and acyl-coA synthase 2 (ACSF2), which initiates fatty acid metabolism (Table S5). The rockfish also up-regulated genes encoding ribosomal proteins (RPL9, RPL23)

and a cathepsin L protease (CATL). The genes down-regulated at 12 h included three variants of sterile alpha motif domain-containing proteins (SAMD9 and SAMD9-like), ribosomal protein L7A, the α subunit of ATP synthase (ATP6), and an interferon-induced very large GTPase (GVIN1).

At 24 h, genes central to aerobic and anaerobic metabolism were up-regulated, including cytochrome c oxidase (COX3), ATP synthase (ATP6), and glyceraldehyde-3-phosphate dehydrogenase (GAPDH) (Table S5). Also up-regulated were troponins, myosins, and titins, genes essential to striated muscle contraction. The genes down-regulated at 24 h included septin-4 (SEPT4), a kinesin-associated protein family NTPase (NKPD1), tubulin α -2 (TBA2), microtubule-associated protein 2 (MAP2), β -galactoside α -2,6-sialyltransferase 2 (SIAT2), a serine/threonine protein kinase (TAOK1), and protein phosphatase slingshot homolog 2 (SSH2) which regulates actin filament construction by activating the depolymerization factor cofilin.

At two weeks of exposure to high $p\text{CO}_2$, we observed up-regulation of more genes than at either 12 h or 24 h, encoding ribosomal proteins (RPL7A, RPL13, RPL19, RPL23, RPL24, RPL30, RPL32), muscular contractile components (light- and heavy-chain myosins, paramyosins, actins and nebulins) and sustained mitochondrial metabolic demand (cytochrome b-c1 complex subunits COX3, CYB, COX4, and UQCRB as well as ATPases and ATP synthases, Table S5). One cytochrome b-c1 complex subunit was down-regulated after two weeks (COX2), as was CKM and three genes involved in the mild cellular stress response: a DNA repair protein (RAD51D), an E3 ubiquitin-protein ligase (RNF213B), and saccin (SACS), which is a co-chaperone for heat-shock protein 70. Among all three time-points, 18 genes whose functions were identified were differentially expressed under high $p\text{CO}_2$. These encoded muscular proteins like myosins, troponins, and SERCA1, key electron transport chain proteins like cytochrome b and c (CYB and COX3), and ATP metabolic proteins like CKM, and ATP synthase (ATP6). In total, we identified the functions of 95 unique genes that blue rockfish differentially expressed in response to high $p\text{CO}_2$ (Table S5).

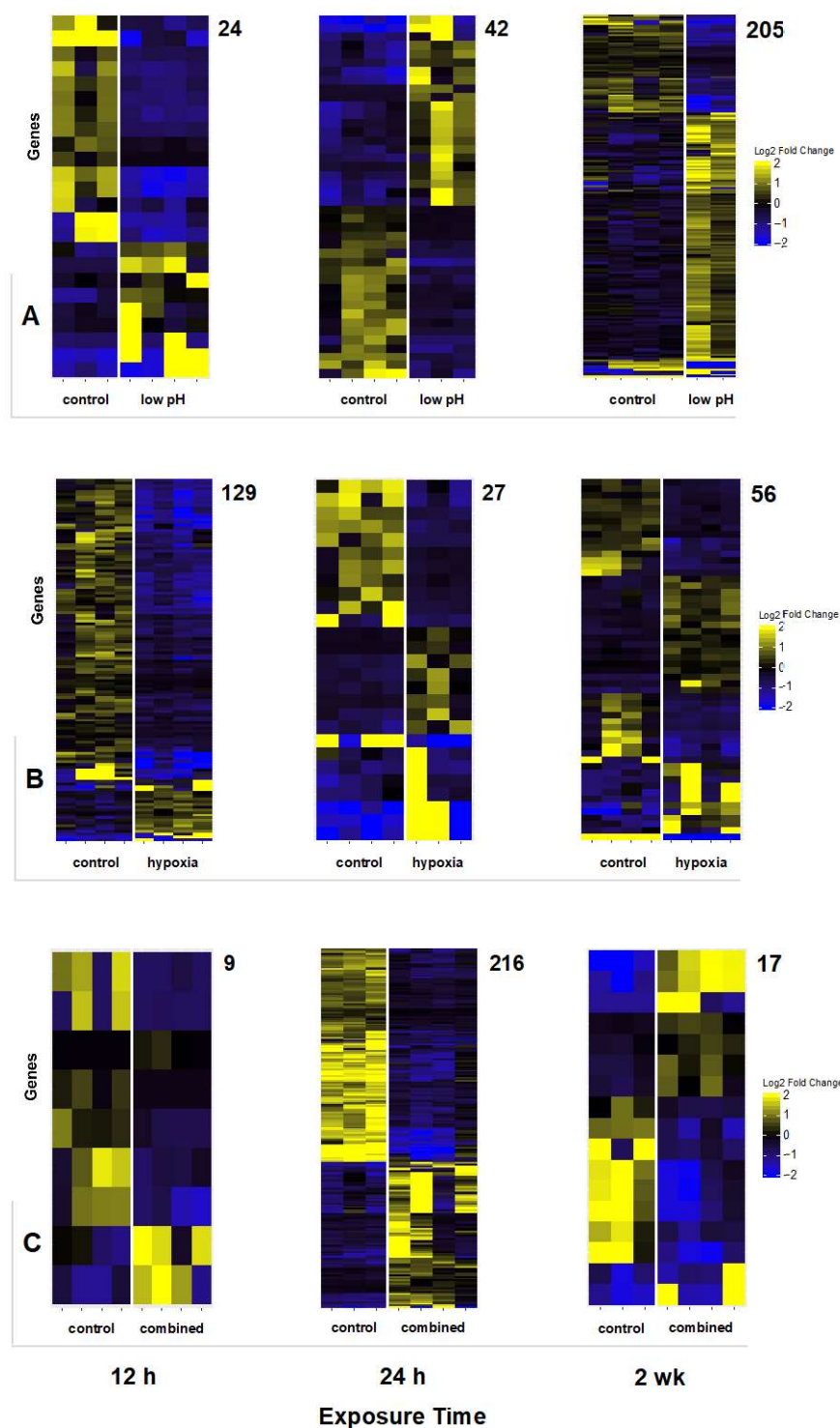


Figure 3: Relative gene expression in control and experimental blue rockfish muscle tissue after 12 h, 24 h and two weeks of exposure to A) high $p\text{CO}_2$ /low pH ($p\text{CO}_2 \sim 1200 \mu\text{atm}$, $\text{pH} \sim 7.6$, $\text{DO} \sim 8.0 \text{ mg/L}$) B) hypoxia ($p\text{CO}_2 \sim 400 \mu\text{atm}$, $\text{pH} \sim 8.0$, $\text{DO} \sim 4.0 \text{ mg/L}$) and C) combined high $p\text{CO}_2$ /hypoxia ($p\text{CO}_2 \sim 1200 \mu\text{atm}$, $\text{pH} \sim 7.6$, $\text{DO} \sim 4.0 \text{ mg/L}$) (FDR < 0.05). Each row represents a gene, while each column represents an individual fish. Numbers listed indicate gene totals in each heatmap. Yellow shades indicate relative up-regulation, while blue shades indicate down-regulation compared to the mean expression level across all samples. Black indicates no change in expression.

Treatment effects over time: hypoxia

Blue rockfish held under hypoxia exhibited different patterns in gene expression than those held under high $p\text{CO}_2$. Overall DE was greatest at 12 h, with 129 genes differentially expressed. Substantially less DE was observed at 24 h (27 genes), while 56 DE genes were observed at the two-week time-point (Figure 2). Only 16 genes were commonly expressed between the hypoxic and high $p\text{CO}_2$ treatments, encoding proteins involved in processes ranging from ATP and fatty acid metabolism (CKM, ATP6, ACSF2 and fatty acid-binding protein FABP2) to muscle contraction (troponin I and SERCA1) to putative control of cellular proliferation (sterile alpha motif domain-containing protein 9 homolog, SAMD9L).

At 12 h in the hypoxic treatment, the 22 up-regulated genes included some of the same metabolic genes observed under high $p\text{CO}_2$ including CKM, COX3, and ACSF2. Also up-regulated at 12 h were carbonic anhydrase 1 (CA1) and two proteins possibly involved in the cellular stress response: nucleoside diphosphate kinase (NDKB) and an E3 ubiquitin-protein ligase (RNF144B). At 12 h, however, the vast majority of the 129 DE genes (107) were down-regulated compared to fish from the control treatment (Figure 3). These down-regulated genes encoded structural proteins like the fast-twitch isoform of troponin I (TNNI2), α -tubulin (TUBA1), microtubule-associated protein 2 (MAP2) as well as transcription factors (CEBPD, ATF1, ATF3, HES1A, LMO41, ALPK3), E3 ubiquitin ligases (TRIM63, MYLIP-A), and certain serine/threonine protein kinases (STK35, NIM1).

At 24 h in the hypoxic treatment, the 15 up-regulated genes included CKM, COX3, SERCA1, and ATP6. The 12 genes down-regulated under hypoxia at 24 h included troponin I (skeletal muscle fast-twitch isoform), transcription factor ATF1, histone H3.2, elongation factor 1-gamma (EF1G) which elongates peptides during translation, and protein phosphatase slingshot homolog 2 (SSH2).

After two weeks under hypoxia, blue rockfish differentially expressed 56 genes (29 up-regulated, 27 down-regulated). Among the up-regulated genes were FABP2, COX3, a hemoglobin subunit (HBB2), metal-binding metallothionein A (MTA), and fructose-bisphosphate aldolase A (ALDOA), a key protein in glycolysis and gluconeogenesis. At all three time-points under hypoxia, one COX3 subunit and at least

one indicator of mild cellular stress were up-regulated (apoptosis regulator RNF144B at 12 h, apoptosis regulator TRIM39 at 24 h and an aldehyde dehydrogenase, P5CS, at two weeks) (Table S5). Across all time-points, we identified the functions of 110 unique genes that blue rockfish differentially expressed in response to hypoxia.

Treatment effects over time: combined high pCO₂ and hypoxia

Under combined high pCO₂ and hypoxia, blue rockfish gene expression profiles differed from those observed under the independent stressors. Differential gene expression was minimal at 12 h and two weeks (9 and 17 genes, respectively), but peaked markedly at 24 h (216 genes) (Figure 2). Most of these genes (128) were down-regulated at the 24 h time-point. At 24 h in the independent high pCO₂ and hypoxic treatments, a total of only 69 DE genes were observed.

At 12 h of exposure to the combined stressors, only nine genes exhibited differential expression relative to fish from the control treatment, three of which were up-regulated and six down-regulated. Two of the up-regulated genes at 12 h were a stonustoxin subunit (STXB) and a long-chain fatty acid-coA ligase (ACBG1), while none of the six down-regulated genes received functional UniProtKB annotations. At 24 h under the combined stressors, blue rockfish dramatically increased DE in their white muscle, up-regulating 88 genes and down-regulating 128 genes for a total of 216 differentially expressed genes. Notably at 24 h, more genes involved in ionoregulation were up-regulated under both stressors than under high pCO₂ or hypoxia alone, including the α -1 and α -3 subunits of a sodium/potassium-transporting ATPase pump (AT1A1, AT1A3), an intracellular chloride channel protein (CLIC2), a HIF-hydroxylating cellular oxygen sensor (EGLN2) and GAPDH (Table S5). Additionally at 24 h, a cellular oxygen sensor (EGLN2) that hydroxylates the α subunits of HIF1 and HIF2 was up-regulated.

After two weeks under both stressors, DE decreased to 17 genes (nine genes up-regulated, eight genes down-regulated). Among the up-regulated genes in this group were two hemoglobin subunits (HBAE, HBB2), carbonic anhydrase (CAHZ), a cytochrome B complex subunit (CYB) and ALDOA, the latter of which is involved in glycolysis. Also at two weeks, the heat shock protein 70-associated protein 13 (HSPA13) was down-regulated. Over all time, we observed 131 different DE genes under combined

high $p\text{CO}_2$ and hypoxia. 104 of these 131 genes were expressed only under the combined stressors and not under independent high $p\text{CO}_2$ or hypoxia. The genes uniquely expressed under the combined stressors were involved in various signaling (insulin/IGF-1, integrin, interleukin, Wnt, Ras, TGF- β , CCKR, and PDGF) and biosynthetic (coenzyme A, vitamin B6 and noradrenaline biosynthesis) pathways (Figure 4).

Finally, we also observed a large increase in the total number of differentially expressed genes in each treatment over time suggesting an effect of laboratory exposure independent of treatment. For example, in the control treatment, over 4,500 genes were differentially expressed between 24 h and two weeks ($\text{FDR} < 0.05$). Thousands of genes were also regulated over time in the other treatments. To isolate the effect of treatment versus time, all previous comparisons were made to the control treatment.

Functional similarities between treatments

Based on numbers of DE genes, we found no evidence of an additive effect of combined high $p\text{CO}_2$ and hypoxia on blue rockfish gene expression, while the presence of synergism or antagonism was heavily dependent on exposure time. Across all time-points, similar numbers of total DE genes observed in the three experimental treatments indicate moderate antagonism between high $p\text{CO}_2$ and hypoxia: 242 genes in the combined treatment compared with 271 genes under high $p\text{CO}_2$ and 212 genes under hypoxia. At 12 h and two weeks of exposure to the combined stressors, we observed strong antagonism in the low numbers of responsive genes (9 and 17, respectively) but comparatively high numbers of DE genes under independent high $p\text{CO}_2$ (24 and 205, respectively) and hypoxia (129 and 56, respectively) at the same time-points (Figure 2). In contrast, a strong synergism was observed at 24 h, with 216 DE genes observed under the combined stressors but only 69 total DE genes between the two independent stressor treatments. There was also qualitative evidence for this synergism in the functionality of some unique genes and GO categories expressed under the combined stressors.

70-78% of the UniProtKB-annotated genes responsive under high $p\text{CO}_2$, hypoxia or the combined stressors were successfully classified into PANTHER pathways. 19 distinct GO pathways were identified under high $p\text{CO}_2$, 20 pathways were identified

under hypoxia, and 33 different pathways were identified under combined high $p\text{CO}_2$ and hypoxia (Figure 4). Of these, eight pathways represented by at least one gene were common to both the independent high $p\text{CO}_2$ and hypoxia treatments. 13 pathways were commonly represented under high $p\text{CO}_2$ and the combined stressors, including the Ras signaling pathway, glycolysis and the oxidative stress response. 15 pathways were represented under hypoxia and the combined stressors. These 15 pathways included integrin signaling, both the p38 microtubule-associated protein kinase (MAPK) and insulin-like growth factor (IGF) MAPK pathways, Wnt signaling and apoptosis signaling. Only seven pathways were represented in all three experimental treatments, including the p38 MAPK pathway, integrin signaling, Wnt signaling, chemokine/cytokine-mediated inflammation, and pathological pathways associated with Parkinson and Huntington diseases. 12 pathways were uniquely represented under combined high $p\text{CO}_2$ and hypoxia. These 12 pathways included the hypoxia response via HIF activation (not observed under independent hypoxia), the PDGF and TGF- β signaling pathways, T-cell activation and various metabolic pathways. No statistically significant over-representation of any GO pathways was observed in any of the three treatments.

Because our annotated DGE lists were relatively short (95-131 genes) and the PANTHER over-representation analysis had low power to detect potential differences, we also manually examined individual gene function among the three experimental groups. Over all time-points, a moderate antagonistic effect was also observed in the numbers of annotated genes expressed in each treatment, with 95 unique genes expressed under high $p\text{CO}_2$, 110 genes unique genes expressed under hypoxia but only 131 unique genes expressed under both stressors. 104 of these 131 genes were expressed only under the combined stressors and not under independent high $p\text{CO}_2$ or hypoxia.

Based on function, there was little similarity among annotated genes differentially expressed among the three experimental treatments at any given time-point (Figure 5). Over all time-points in the independent high $p\text{CO}_2$ and hypoxic treatments, 16 annotated genes out of 189 unique annotated DE genes were commonly differentially expressed (23 common contigs out of 445 unique contigs, including two isoforms of CKM). At 12 h, CKM, ACSF2, and ribosomal protein L9 were commonly up-regulated under the two independent stressors. At 24 h, COX3, ATP6, troponin I and an uncharacterized protein

(ART2) were also all up-regulated under high $p\text{CO}_2$ and hypoxia. Also at 24 h, protein phosphatase slingshot homolog 2 (SSH2) was down-regulated in both treatments.

Over all time under both high $p\text{CO}_2$ and the combined stressors, 10 annotated genes out of 216 unique annotated DE genes were commonly differentially expressed (16 common contigs out of 487 unique contigs). GAPDH, a known glycolytic enzyme, was commonly up-regulated under high $p\text{CO}_2$ and the combined stressors at 24 h. Also at 24 h, septin-4 and β -galactoside α -2,6-sialyltransferase 2 were commonly down-regulated.

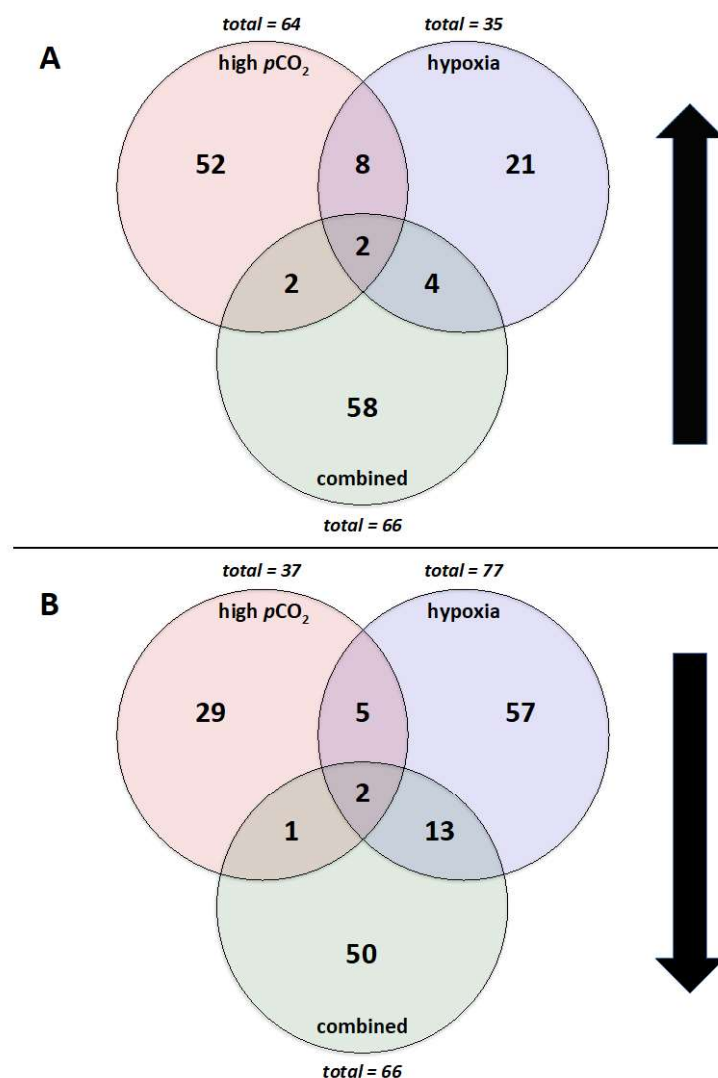


Figure 5: A) Up-regulated genes and B) down-regulated genes in blue rockfish white muscle under high $p\text{CO}_2$, hypoxia and combined high $p\text{CO}_2$ /hypoxia versus the control treatment (FDR<0.05) and annotated against the UniProtKB protein database.

At two weeks, SERCA1 was up-regulated in both treatments.

Under both hypoxia and the combined stressors, 22 annotated genes out of 219 unique annotated DE genes were commonly differentially expressed (33 common contigs out of 410 unique contigs). 13 of the 22 shared genes were down-regulated at both 12 h under hypoxia and 24 h under the combined stressors, coinciding with the large numbers of down-regulated genes in the hypoxic and combined treatments at these time-points. 10 of the 13 shared genes were involved in signaling pathways including the apoptosis,

insulin/IGF-1, interleukin, ionotropic and metabotropic glutamate receptor pathways. At 24 h, elongation factor 1-gamma was down-regulated under both hypoxia and the combined stressors. At 24 h, cysteine and glycine-rich protein 1 (CSRP1) was up-regulated under hypoxia and the combined stressors. At two weeks, a hemoglobin subunit (HBB2) and muscle-specific fructose-bisphosphate aldolase A (ALDOA, involved in glycolysis) were commonly up-regulated under hypoxia and the combined stressors at two weeks.

Among all three experimental treatments across all three time-points, there were only 6 unique contigs in common (out of 641), 5 of which were annotated. One of these five, SERCA1, was exclusively up-regulated. SERCA1 was up-regulated at 12 h and two weeks under high $p\text{CO}_2$, at 24 h under hypoxia and at two weeks under the combined stressors. SERCA1 and CKM were up-regulated in all three treatments. CKM was the most frequently occurring gene and was up-regulated in all three treatments at either 12 h or 24 h. CKM was also down-regulated at two weeks under both independent high $p\text{CO}_2$ and hypoxia. Two genes were exclusively down-regulated (septin-4 and β -galactoside α -2,6-sialyltransferase 2) under high $p\text{CO}_2$ and the combined stressors at 24 h, as well as under hypoxia at 12 h.

METABOLIC ENZYME ACTIVITY ASSAYS

We observed no statistically significant effect of treatment on either LDH activity or CS activity in blue rockfish muscle, gill or liver. In blue rockfish liver tissue, we observed a significant decrease in LDH (anaerobic) activity between 24 h and two weeks, but not between the control and combined high $p\text{CO}_2$ /hypoxia treatments at any time-point (Two-way ANOVA, $p=0.001$, Tukey *post hoc*, Figure 6). In gill tissue, we observed increases in CS (aerobic) activity between 24 h and two weeks, but not between the control and experimental treatments (Two-way ANOVA, $p=0.0003$, Tukey *post hoc*, Figure 7). Normalizing enzyme activities to grams fresh protein (GFP) yielded the same statistical results when compared to activities normalized to grams fresh weight of tissue (GFW), and therefore we only present results normalized to GFW. LDH activities in blue rockfish gill tissue were not normally distributed per a Shapiro-Wilk test ($p=0.0003$), so

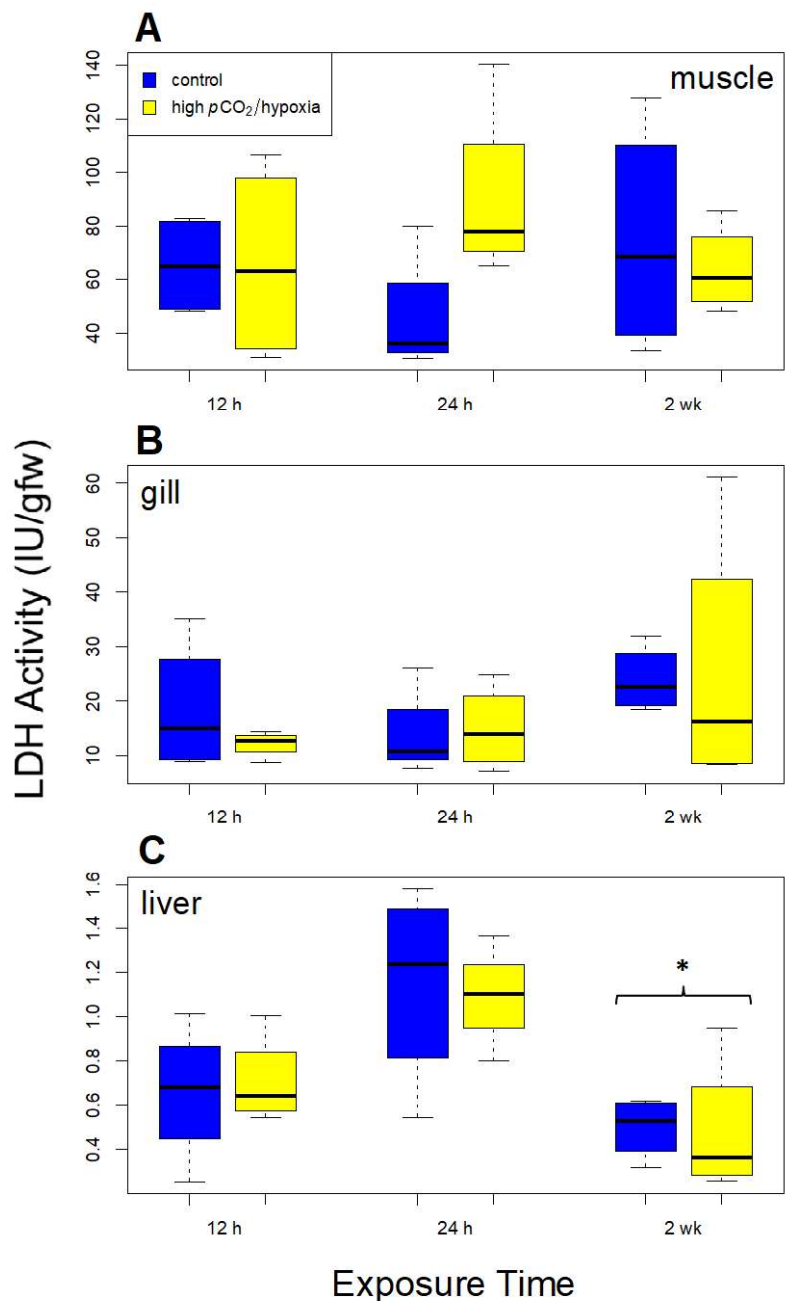


Figure 6: Lactate dehydrogenase (LDH) enzyme activity in blue rockfish A) white muscle B) gill and C) liver tissues after 12 h, 24 h and two weeks of exposure to either control or combined high $p\text{CO}_2$ /hypoxic conditions. Enzyme activities were normalized to grams fresh weight of tissue (GFW). Asterisks (*) indicate significant differences between 24 h and two weeks in liver ($p=0.001$), but not between treatments (two-way ANOVA, Tukey pairwise *post hoc*). A Box-Cox transformation was applied to the gill tissue LDH activity prior to ANOVA testing due to non-normality.

we applied a Box-Cox transformation to the gill tissue LDH activities before two-way ANOVA testing ($\lambda_{\text{LDH}} = -0.9436$). Importantly, we observed no statistically significant differences between the control and combined stressor treatments at any time-point. Anaerobic (LDH) activities were greatest overall in blue rockfish white muscle (Figure 6), while the greatest aerobic (CS) activities were observed in gill tissue (Figure 7). Liver tissue consistently exhibited the lowest LDH activities (Figure 7).

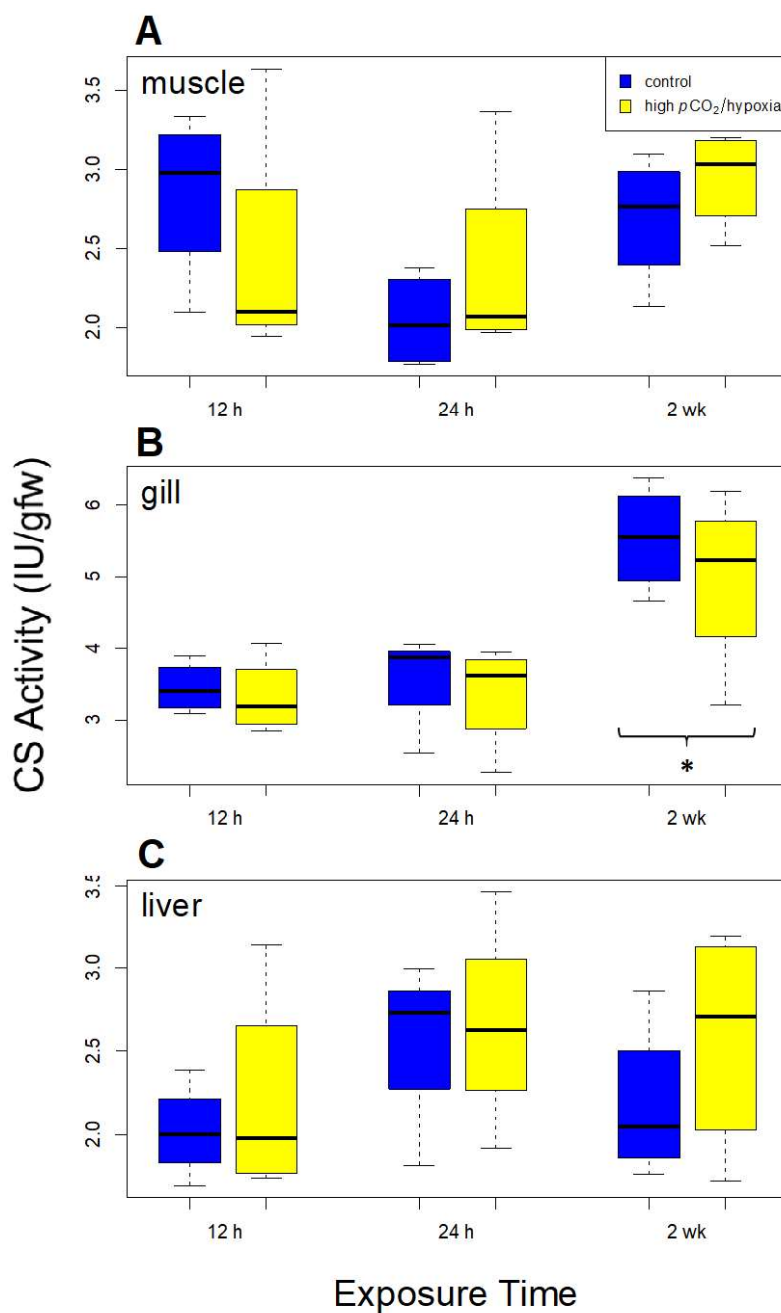


Figure 7: Citrate synthase (CS) enzyme activity in blue rockfish A) white muscle B) gill and C) liver tissues after 12 h, 24 h and two weeks of exposure to either control or combined high $p\text{CO}_2$ /hypoxic conditions. Enzyme activities were normalized to grams fresh weight of tissue (GFW). Asterisks (*) indicate significant differences between 24 h and two weeks in gill ($p=0.0003$), but not between treatments (two-way ANOVA, Tukey pairwise *post hoc*).

SECTION 4

DISCUSSION

Previous studies suggest that blue rockfish may be relatively tolerant to the effects of climate change compared with other rockfish congeners (Fennie 2015, Hamilton et al. 2017). In this study, we examined the molecular mechanisms by which blue rockfish respond to climate related stressors over acute and acclimatory timescales. We also examined whether there was an interactive effect between hypoxia and high $p\text{CO}_2$ by comparing responses to the individual stressors to those from a combined stressor treatment. Exposure to combined high $p\text{CO}_2$ and hypoxia better simulates exposure to intensified upwelling conditions expected with climate change. We found that genes responsive to the combined stressors of high $p\text{CO}_2$ /hypoxia were mostly unique compared to the individual stressors alone, but that there were also some shared responses between the combined and individual stressor treatments. We observed both novel and previously known transcriptional responses to high $p\text{CO}_2$ and hypoxia. However, we found no evidence of a shift towards anaerobic metabolism or a sustained cellular stress response (CSR) over the time-course, providing additional evidence that blue rockfish may be relatively tolerant to the effects of future climate change.

INTERACTIVE RESPONSES TO HIGH $p\text{CO}_2$ AND HYPOXIA

Rockfishes are frequently exposed to multiple stressors in their natural environment and have evolved physiological and molecular adaptations to respond. The mechanisms of cross-talk between responses that are unique to individual stressors versus those that are shared are not well characterized. We hypothesized that gene expression under combined high $p\text{CO}_2$ and hypoxia would reflect the same genes responsive to the individual stressors, yielding an additive response. We also noted the possibility of physiological responses to each single stressor interacting synergistically (e.g. respiratory acidosis as increased ventilation rates under low DO and low pH exchange more CO_2 through the gills, or exacerbated metabolic stress as fish decrease ventilation under low

DO to avoid acidosis) and in turn inducing DE of novel gene groups not observed under the individual stressors (Vulesevic et al. 2006, Esbaugh et al. 2012, Heuer and Grosell 2014, Miller et al. 2016, Esbaugh 2018). Under this framework, we identified genes and pathways unique to each treatment as well as shared responses between the stressors.

We found no evidence for a purely additive interaction between high $p\text{CO}_2$ and hypoxia at any time-point, but observed evidence of synergism at 24 h of exposure. Greater overall DGE (216 genes) was observed at this time-point than in either of the independent treatments (42 genes under high $p\text{CO}_2$ and 27 genes under hypoxia), including representation of all 33 GO pathways observed in the combined treatment across the time-course. This response was not evident at two weeks, however. It is possible that an early, coordinated synergistic response that altered various signaling pathways allowed the fishes to acclimate by two weeks. The sustained DGE at two weeks under both independent high $p\text{CO}_2$ and independent hypoxia, however suggests a strongly antagonistic relationship between the two stressors.

Under the combined stressors, hypoxia appeared to dominate the response of blue rockfish. The greatest number of shared GO pathways (15) was shared between the hypoxic and combined stressor treatments. Many of these were signaling pathways that may have stimulated downstream protein expression and arrival at a muscular phenotype more suited to a hypoxic environment. Similar to the immediate down-regulation of 107 genes under hypoxia at 12 h, at 24 h under the combined stressors we observed down-regulation of 128 genes including transcription factors, cytoskeletal components and ribosomal proteins that may indicate a slowing of overall metabolism and protein turnover (Gracey et al. 2001).

Also at 24 h, blue rockfish began to exhibit some signs of acclimation to the combined stressors. Unexpected down-regulation of a number of CSR-induced genes such as polyubiquitin B and H, two DNA damage-inducible repair proteins (SPIDR and DDT4L), and heat shock factor protein 4 (HSF4) at 24 h could represent acclimation to the stressors. Additional evidence for acclimation to the combined stressors at 24 h was up-regulation of a cellular oxygen sensor (EGLN2) that hydroxylates the α subunits of HIF1 and HIF2. Hydroxylated HIFs are typically marked for proteosomal degradation, hence the up-regulation of EGLN2 at 24 h may represent targeted elimination of HIFs

used to stimulate an early hypoxia response that was not captured at the mRNA level. At two weeks under the combined stressors, the heat shock protein 70-associated protein 13 (HSPA13) was down-regulated, possibly indicating a diminished need for protein chaperone activity.

While few genes were differentially expressed at two weeks under combined high $p\text{CO}_2$ and hypoxia, the genes up-regulated at this time-point suggest that multiple compensatory responses were engaged: two hemoglobin subunits (HBAE and HBB2) may indicate increased erythropoiesis, the important glycolytic fructose-bisphosphate aldolase A (ALDOA) may indicate an increased reliance on glycolysis, and carbonic anhydrase (CAHZ) may indicate lasting ionoregulatory shifts under the combined stressors (Table S5).

TRANSCRIPTOMIC RESPONSES TO HIGH $p\text{CO}_2$ AND HYPOXIA OVER TIME

We predicted that elevated $p\text{CO}_2$ would stimulate DE of ionoregulatory, muscular contractile and metabolic genes in blue rockfish. We observed a steady increase in overall DGE over two weeks, characterized by up-regulation of key metabolic genes as well as muscular and cytoskeletal structural components, but no accompanying ionoregulatory shifts. At 12 h, when compared to control fish, blue rockfish immediately increased expression of genes encoding proteins involved in metabolic ATP demand, up-regulating energy-transducing proteins like creatine kinase m-type (CKM), sarcoplasmic reticulum calcium ATPase 1 (SERCA1), and acyl-coA synthase 2 (ACSF2), which initiates fatty acid metabolism. At 24 h, the fishes up-regulated genes central to aerobic and anaerobic metabolism such as cytochrome c oxidase (COXC), ATP synthase, and GAPDH. They also up-regulated troponins, myosins, and titins, genes essential to striated muscle contraction. Interestingly, Hamilton et al. (2017) observed down-regulation of these components in blue rockfish muscle at higher $p\text{CO}_2$ levels (2800 μatm), suggesting plasticity in muscle composition in response to different levels of $p\text{CO}_2$.

At two weeks of exposure to high $p\text{CO}_2$, we observed a response of greater magnitude than at either 12 h or 24 h. Up-regulated genes included those involved in increased protein synthesis (ribosomal proteins RPL7A, RPL13, RPL19, RPL23, RPL24,

RPL30, RPL32), muscular restructuring (light- and heavy-chain myosins, paramyosins, actins and nebulins) and sustained metabolic demand (cytochrome b and c oxidases, ATPases and ATP synthases). A recent study of the muscle proteome of sea bream (*Sparus aurata*) after 42 days under a pH of 7.5 reported up-regulation of proteins involved in many of these same categories including glycolysis and lipid metabolism (Araújo et al. 2018), suggesting utilization of these energetic pathways in the muscle tissue of some teleosts under OA.

We observed that over acute timescales (12-24 h), hypoxia stimulated substantial down-regulation of transcriptional and signaling machinery under independent hypoxia (12 h) and combined high $p\text{CO}_2$ /hypoxia (24 h). Perhaps the most significant DE pattern in the hypoxic condition was an immediate down-regulation at 12 h of 107 genes involved in signaling, muscle structure, and transcriptional regulation. These patterns may indicate targeted changes in transcription and decreased protein synthesis/turnover in blue rockfish under low DO, which are known ATP conservation strategies (Liu and Simon 2004). Interestingly, few of these down-regulated genes were involved in protein biosynthesis, even though protein synthesis is one of the most energetically costly cellular processes and often leads to strong down-regulation of ribosomal subunits and other translation machinery (Gracey et al. 2001, Ton et al. 2003). The strong down-regulation of transcription factors may indicate that reductions in protein synthesis were more targeted at the transcriptional level. Separately, down-regulation of monocarboxylate transporter 10 (MCT10) at 12 h represented an expression pattern opposite that of MCT4 observed over a chronic timescale in the zebrafish (*Danio rerio*) (van der Meer et al. 2005). MCTs aid in the transport of glycolytic metabolites like pyruvate and lactate, and thus the function of these proteins under hypoxia may change with the duration of reliance on glycolysis.

Under hypoxia, we also expected to observe DE of genes involved in conserved vertebrate hypoxia responses like a mild CSR, glycolysis, erythropoiesis and/or angiogenesis, and altered expression of oxygen sensors like HIFs and prolyl hydroxylases (PHDs) or their downstream targets (Xiao 2015). We observed expression of few of these genes, however, but observed up-regulation of carbonic anhydrase (CA1). Recent evidence suggests that CA1 may be hypoxia-induced and mediate dissociation of O_2 from

hemoglobin by altering extracellular pH in fish (Randall 1982, Esbaugh et al. 2008, Alderman et al. 2016). Up-regulation of these ionoregulatory genes did not continue at two weeks, suggesting that the fish underwent osmotic shifts early in the time course to account for increased ventilation or another method of oxygen delivery. After two weeks under hypoxia, blue rockfish also up-regulated a hemoglobin subunit (HBB2) in their white muscle, possibly indicating heightened erythrocyte production. These findings indicate that blue rockfish contended with moderate hypoxia through multiple responses, one of which may involve a change in ionoregulatory status to alter the affinity of oxygen-carrying molecules and release O₂ that would otherwise be unavailable.

Unexpectedly, our data also revealed a large effect of time on gene expression in blue rockfish muscle tissue in this experiment across all treatments, including the control. For example, between 24 h and two weeks, more than 4,500 genes were differentially expressed. This could have been a result of handling stress or an acclimatory response to the experimental set-up. Previous studies have also noted strong effects of routine handling and husbandry on the composition of skeletal muscle in teleosts (Aedo et al. 2015). Over longer-term periods in the laboratory, blue rockfish are known to have lower survival rates than other rockfish species even under ambient conditions (Mattiasen 2018). Although we cannot explain what drove the large changes in gene expression over time, we highlight the importance of sampling control fish at every time-point during a time course experiment to remove the effect of time from treatment-driven responses.

RELATIVE RESILIENCE OF BLUE ROCKFISH AT THE MOLECULAR LEVEL

Our findings suggest that blue rockfish may be physiologically equipped to cope with moderately elevated $p\text{CO}_2$ (~1200 μatm) and moderate levels of hypoxia (~4.0 mg O₂/L) during upwelling. In combination, the two stressors did not induce a shift towards anaerobic metabolism based on metabolic enzyme activities nor did they result in any mortality. Similarly, we did not observe significant differential expression of citrate synthase or lactate dehydrogenase isoforms or subunits in the muscle tissue gene expression data, but it is possible that genes encoding these proteins were differentially regulated in the gills, liver or other tissues.

At the transcriptomic level under the combined stressors, we observed few signs of a CSR under the combined stressors. These findings contrast with a study in *Trematomus bernachii* gill tissue that observed an acute CSR persisting for seven days in response to high $p\text{CO}_2$ (1000 μatm) and warming (+4° C) (Huth and Place 2016). Like *T. bernachii*, however, blue rockfish did not exhibit an inducible CSR or heat shock response to independent high $p\text{CO}_2$ (Huth and Place 2016). We note that the threshold levels of $p\text{CO}_2$ and hypoxia for this species may lie below the levels to which the fishes were exposed in this experiment (Vaquer-Sunyer and Duarte 2008). Given that OA and hypoxia are predicted to become more prevalent in the CCLME, the wide range of sensitivities across taxa and the possibility that native organisms are already living close to their physiological limits, we highlight the importance of species-specific studies in the context of multiple stressors (Crain et al. 2008, Vaquer-Sunyer and Duarte 2008, Monaco and Helmuth 2011).

CONCLUSION

We found that juvenile blue rockfish differentially expressed largely dissimilar gene suites under independent high $p\text{CO}_2$, independent hypoxia and combined high $p\text{CO}_2$ and hypoxia. Among the mechanisms employed by blue rockfish to contend with high $p\text{CO}_2$ and hypoxia were cytoskeletal restructuring, the activation of glycolysis and fatty acid metabolism, increased hemoglobin production, and altered ionoregulation, possibly for the purpose of maintaining O_2 -hemoglobin affinity while buffering against hypercapnia. Interestingly, under the combined stressors, a synergistic spike in DGE at 24 h allowed for a relaxation in DGE at two weeks. The absence of a significant CSR or increased enzymatic reliance on anaerobic metabolism indicates that blue rockfish may be physiologically resistant to moderate levels of $p\text{CO}_2$ and hypoxia.

Even if blue rockfish are resistant to moderate high $p\text{CO}_2$ and hypoxia, additional studies in this and other native rockfish species are required to inform the larger groundfish fishery in central California. Previous work has suggested differential tolerances among congeners within *Sebastes*, which could influence the composition of juvenile rockfish assemblages that are an important mid-trophic food source for predatory

fishes and seabirds (Hamilton *et al.* 2017, Davis *et al.* 2018, Warzybok *et al.* 2018). Knowledge of the mechanisms that rockfish employ to contend with ocean acidification and hypoxia (particularly at critical life stages) may help interpret future shifts in populations or catch totals (Young *et al.* 2006, Metcalfe *et al.* 2012). Future research should address the possibility of species-specific thresholds under these stressors, above or below which species are impacted even if negative effects are not observed at less severe levels of the stressor(s) (Vaquer-Sunyer and Duarte 2008, Hamilton *et al.* 2017). The use of fluctuating $p\text{CO}_2$ and DO levels should also be considered in lieu of static exposures, in order to better emulate the onset of upwelling events and to capture physiological or behavioral patterns (i.e. recovery) that may not be observed under static $p\text{CO}_2$ and DO (Brady and Targett 2010, Booth *et al.* 2012, Jarrold *et al.* 2017). In aggregate, this information may inform the condition or recruitment success of different rockfishes under extreme oceanographic conditions in the Northeast Pacific such as increasingly strong upwelling events.

REFERENCES

- Aedo, J.E., Maldonado, J., Aballai, V., Estrada, J.M., Bastias-Molina, M., Meneses, C. & Valdés, J.A. (2015). mRNA-seq reveals skeletal muscle atrophy in response to handling stress in a marine teleost, the red cusk-eel (*Genypterus chilensis*). *BMC Genomics*, 16(1), 1-12.
- Alderman, S.L., Harter, T.S., Wilson, J.M., Supuran, C.T., Farrell, A.P. & Brauner, C.J. (2016). Evidence for a plasma-accessible carbonic anhydrase in the lumen of salmon heart that may enhance oxygen delivery to the myocardium. *Journal of Experimental Biology*, 219(5), 719-724.
- Araújo, J.E., Madeira, D., Vitorino, R., Repolho, T., Rosa, R. & Diniz, M. (2018). Negative synergistic impacts of ocean warming and acidification on the survival and proteome of the commercial sea bream, *Sparus aurata*. *Journal of Sea Research*, 139, 50-61.
- Bakun, A. (1990). Global Climate Change and Intensification of Coastal Ocean Upwelling. *Science*, 247(4939), 198-201.
- Bakun, A., Black, B.A., Bograd, S.J., García-Reyes, M., Miller, A.J., Rykaczewski, R.R. & Sydeman, W.J. (2015). Anticipated Effects of Climate Change on Coastal Upwelling Ecosystems. *Current Climate Change Reports*, 1(2), 85-93.
- Bograd, S.J., Castro, C.G., Di Lorenzo, E., Palacios, D.M., Bailey, H., Gilly, W. & Chavez, F.P. (2008). Oxygen declines and the shoaling of the hypoxic boundary in the California Current. *Geophysical Research Letters*, 35(12), 1-6.
- Bolger, A.M., Lohse, M. & Usadel, B. (2014). Trimmomatic: A flexible trimmer for Illumina Sequence Data. *Bioinformatics*, 30(15), 2114-2120.
- Booth, J.A.T., McPhee-Shaw, E.E., Chua, P., Kingsley, E., Denny, M., Phillips, R., Bograd, S.J., Zeidberg, L.D. & Gilly, W.F. (2012). Natural intrusions of hypoxic, low pH water into nearshore marine environments on the California coast. *Continental Shelf Research*, 45, 108-115.
- Brady, R.X., Alexander, M.A., Lovenduski, N.S. & Rykaczewski, R.R. (2017). Emergent anthropogenic trends in California Current upwelling. *Geophysical Research Letters*, 44(10), 5044-5052.
- Breitburg, D., Levin, L.A., Oschlies, A., Grégoire, M., Chavez, F.P., Conley, D.J., Garçon, V., Gilbert, D., Gutiérrez, D., Isensee, K., Jacinto, G.S., Limburg, K.E., Montes, I., Naqvi, S.W.A., Pitcher, G.C., Rabalais, N.N., Roman, M.R., Rose, K.A.,

- Seibel, B.A., Telszewski, M., Yasuhara, M. & Zhang, J. (2018). Declining oxygen in the global ocean and coastal waters. *Science*, 359, eaam7240.
- Buchfink, B., Xie, C. & Huson, D.H. (2015). Fast and sensitive protein alignment using DIAMOND. *Nature Methods*, 12, 59-60.
- Cameron, J.N. (1978). Regulation of blood pH in teleost fish. *Respiration Physiology*, 33, 129-144.
- Cameron, J.N. & Iwama, G.K. (1989). Compromises between ionic regulation and acid-base regulation in aquatic animals. *Canadian Journal of Zoology*, 67, 3078-3084.
- Cattano, C., Claudet, J., Domenici, P. & Milazzo, M. (2018). Living in a high CO₂ world: a global meta-analysis shows multiple trait-mediated fish responses to ocean acidification. *Ecological Monographs*, 88(3), 320-335.
- Chabot, D. & Claireaux, G. (2008). Environmental hypoxia as a metabolic constraint on fish: The case of Atlantic cod, *Gadus morhua*. *Marine Pollution Bulletin*, 57(6-12), 287-294.
- Chan, F., Barth, J.A., Lubchenco, J., Kirincich, A., Weeks, H., Peterson, W.T. & Menge, B.A. (2008). Emergence of anoxia in the California Current Large Marine Ecosystem. *Science*, 319(5865), 920.
- Cheung, W.W.L., Lam, V.W.Y., Sarmiento, J.L., Kearney, K., Watson, R., Zeller, D. & Pauly, D. (2010). Large-scale redistribution of maximum fisheries catch potential in the global ocean under climate change. *Global Change Biology*, 16, 24-25.
- Childress, J. J. & Somero, G. N. (1990). Metabolic scaling: A new perspective based on scaling of glycolytic enzyme activities. *Integrative and Comparative Biology*, 30(1), 161-173.
- Côté, I.M., Darling, E.S. & Brown, C.J. (2016). Interactions among ecosystem stressors and their importance in conservation. *Proceedings of the Royal Society B: Biological Sciences*, 283(1824), 1-9.
- Crain, C.M., Kroeker, K.J. & Halpern, B.S. (2008). Interactive and cumulative effects of multiple human stressors in marine systems. *Ecology Letters* 11, 1304-1315.
- Davidson, M.I., Targett, T.E. & Gre cay, P.A. (2016). Evaluating the effects of diel-cycling hypoxia and pH on growth and survival of juvenile summer flounder *Paralichthys dentatus*. *Marine Ecology Progress Series*, 556, 223-235.
- Davis, B.E., Komoroske, L.M., Hansen, M.J., Poletto, J.B., Perry, E.N., Miller, N.A., Ehlman, S.M., Wheeler, S.G., Sih, A., Todgham, A.E. & Fangue, N.A. (2018).

- Juvenile rockfish show resilience to CO₂-acidification and hypoxia across multiple biological scales. *Conservation Physiology*, 6(1), 1-19.
- Deigweiher, K., Koschnick, N., Pörtner, H.O. & Lucassen, M. (2008). Acclimation of ion regulatory capacities in gills of marine fish under environmental hypercapnia. *American Journal of Physiology: Regulatory, Integrative & Comparative Physiology*, 295, R1660-R1670.
- Dennis, C.E., Kates, D.F., Noatch, M.R. & Suski, C.D. (2015). Molecular responses of fishes to elevated carbon dioxide. *Comparative Biochemistry and Physiology - Part A: Molecular and Integrative Physiology*, 187, 224-231.
- DePasquale, E., Baumann, H. & Gobler, C.J. (2015). Vulnerability of early life stage Northwest Atlantic forage fish to ocean acidification and low oxygen. *Marine Ecology Progress Series*, 523, 145-156.
- Dick, E.J., Berger, A., Bizzarro, J., Bosley, K., Cope, J., Field, J., Gilbert-Horvath, L., Grunloh, N., Ivens-Duran, M., Miller, R., Privitera-Johnson, K. & Rodomsky, B.T. (2017). *The Combined Status of Blue and Deacon Rockfishes in U.S. Waters off California and Oregon in 2017*. Pacific Fishery Management Council, Portland, OR.
- Dickson, A.G., Sabine, C.L. & Christian, J.R. (2007). *Guide to best practices for ocean CO₂ measurements*. PICES Special Publication 3, 191.
- Edgar, R., Domrachev, M. & Lash, A.E. (2002). Gene Expression Omnibus: NCBI gene expression and hybridization array data repository. *Nucleic Acids Research* 30, 207-210.
- Eklblom, R. & Galindo, J. (2011). Applications of next generation sequencing in molecular ecology of non-model organisms. *Heredity*, 107(1), 1-15.
- Ellisdon, A.M., Reboul, C.F., Panjekar, S., Huynh, K., Oellig, C.A., Winter, K.L., Dunstone, M.A., Hodgson, W.C., Seymour, J., Dearden, P.K., Tweten, R.K., Whisstock, J.C. & McGowan, S. (2015). Stonefish toxin defines an ancient branch of the perforin-like superfamily. *Proceedings of the National Academy of Sciences*, 112(50), 15360-15365.
- Enzor, L.A., Zippay, M.L. & Place, S.P. (2013). High latitude fish in a high CO₂ world: synergistic effects of elevated temperature and carbon dioxide on the metabolic rates of Antarctic notothenioids. *Comparative Biochemistry and Physiology - Part A: Molecular and Integrative Physiology*, 164, 154-161.
- Esbaugh, A.J., Perry, S.F. & Gilmour, K.M. (2008). Hypoxia-inducible carbonic

anhydrase IX expression is insufficient to alleviate intracellular metabolic acidosis in the muscle of zebrafish, *Danio rerio*. *American Journal of Physiology: Regulatory, Integrative & Comparative Physiology*, 296(1), R150-R160.

- Esbaugh, A.J., Heuer, R. & Grosell, M. (2012). Impacts of ocean acidification on respiratory gas exchange and acid-base balance in a marine teleost, *Opsanus beta*. *Journal of Comparative Physiology B: Biochemical, Systemic, and Environmental Physiology*, 182(7), 921-934.
- Esbaugh, A.J. (2018). Physiological implications of ocean acidification for marine fish: emerging patterns and new insights. *Journal of Comparative Physiology B: Biochemical, Systemic, and Environmental Physiology*, 188(1), 1-13.
- Fabry, V.J., Seibel, B.A., Feely, R.A. & Orr, J.C. (2008). Impacts of ocean acidification on marine fauna and ecosystem processes. *ICES Journal of Marine Science*, 65, 414-432.
- Feely, R.A., Sabine, C.L., Hernandez-Ayon, J.M., Ianson, D. & Hales, B. (2008). Evidence for upwelling of corrosive “acidified” water onto the continental shelf. *Science*, 320(5882), 1490-1492.
- Fennie, H.W. (2015). “Early life history traits influence the effects of ocean acidification on the behavior and physiology of juvenile rockfishes in central California.” Master of Science Thesis Defense (unpublished), Moss Landing Marine Laboratories, Moss Landing, CA.
- Frable, B.W., Wagman, D.W., Frierson, T.N., Aguilar, A. & Sidlauskas, B.L. (2015). A new species of *Sebastes* (Scorpaeniformes: Sebastidae) from the northeastern Pacific, with a redescription of the blue rockfish, *S. mystinus* (Jordan and Gilbert, 1881). *Fishery Bulletin*, 113(4), 355-357.
- Frieder, C.A., Nam, S.H., Martz, T.R. & Levin, L.A. (2012). High temporal and spatial variability of dissolved oxygen and pH in a nearshore California kelp forest. *Biogeosciences*, 9(10), 3917-3930.
- Fuzzen, M.L.M., Alderman, S.L., Bristow, E.N. & Bernier, N.J. (2011). Ontogeny of the corticotropin-releasing factor system in rainbow trout and differential effects of hypoxia on the endocrine and cellular stress responses during development. *General and Comparative Endocrinology*, 170, 604-612.
- Garcia, T.I., Shen, Y., Crawford, D., Oleksiak, M.F., Whitehead, A. & Walter, R.B. (2012). RNA-Seq reveals complex genetic response to deepwater horizon oil release in *Fundulus grandis*. *BMC Genomics*, 13(1), 1-9.
- Gilmour, K.M. (2001). The CO₂/pH ventilatory drive in fish. *Comparative Biochemistry and Physiology - Part A: Molecular and Integrative Physiology*, 130, 219-240.

- Gilmour, K.M. (2007). Branchial chemoreceptor regulation of cardiorespiratory function. In: *Fish Physiology*, edited by Hara T and Zielinski B. San Diego, CA: 97-151.
- Gobler, C.J., DePasquale, E.L., Griffith, A.W., & Baumann, H. (2014). Hypoxia and acidification have additive and synergistic negative effects on the growth, survival, and metamorphosis of early life stage bivalves. *PLOS ONE*, 9(1), e83648.
- Gobler, C.J. & Baumann, H. (2016). Hypoxia and acidification in ocean ecosystems: Coupled dynamics and effects on marine life. *Biology Letters*, 12(5), 20150976.
- Goolish, E.M. (1991). Aerobic and anaerobic scaling in fish. *Biological Reviews*, 66, 33-56.
- Grabherr, M.G., Haas, B.J., Yassour, M., Levin, J.Z., Thompson, D.A., Amit, I., Adiconis, X., Fan, L., Raychowdhury, R., Zeng, Q., Chen, Z., Mauceli, E., Hacohen, N., Gnirke, A., Rhind, N., di Palma, F., Birren, B.W., Nusbaum, C., Lindblad-Toh, K., Friedman, N. & Regev, A. (2011). Full-length transcriptome assembly from RNA-Seq data without a reference genome. *Nature Biotechnology*, 29, 644.
- Gracey, A.Y., Troll, J.V. & Somero, G.N. (2001). Hypoxia-induced gene expression profiling in the euryoxic fish *Gillichthys mirabilis*. *Proceedings of the National Academy of Sciences*, 98(4), 1993-1998.
- Haas, B.J., Papanicolaou, A., Yassour, M., Grabherr, M., Blood, P.D., Bowden, J., Couger, M.B., Eccles, D., Li, B., Lieber, M., MacManes, M.D., Ott, M., Orvis, J., Pochet, N., Strozzi, F., Weeks, N., Westerman, R., William, T., Dewey, C.N., Henschel, R., LeDuc, R.D., Friedman, N. & Regev, A. (2013). *De novo* transcript sequence reconstruction from RNA-seq using the Trinity platform for reference generation and analysis. *Nature Protocols*, 8, 1494-1512.
- Hamilton S.L., Logan, C.A., Fennie, H.W., Sogard, S.M., Barry, J.P., Makukhov, A.D., Tobosa, L.R., Boyer, K., Lovera, C.F. & Bernardi, G. (2017). Species-specific responses of juvenile rockfish to elevated $p\text{CO}_2$: from behavior to genomics. *PLOS ONE*, 12(1), e0169670.
- Heuer, R.M. & Grosell, M. (2014). Physiological impacts of elevated carbon dioxide and ocean acidification on fish. *American Journal of Physiology: Regulatory, Integrative & Comparative Physiology*, 307(9), R1061-R1084.
- Hoegh-Guldberg, O. & Bruno, J.F. (2010). The impact of climate change on the world's marine ecosystems. *Science*, 328, 1523-1528.
- Huth, T.J. & Place, S.P. (2016). Transcriptome wide analyses reveal a sustained cellular stress response in the gill tissue of *Trematomus bernacchii* after acclimation to multiple stressors. *BMC Genomics*, 17(1), 1-18.

- IPCC, 2014: Climate Change 2014: Synthesis Report. Contribution of Working Groups I, II and III to the Fifth Assessment Report of the Intergovernmental Panel on Climate Change [Core Writing Team, R.K. Pachauri and L.A. Meyer (eds.)]. IPCC, Geneva, Switzerland, 151 pp.
- Jutfelt, F. & Hedgärde, M. (2013). Atlantic cod actively avoid CO₂ and predator odour, even after long-term CO₂ exposure. *Frontiers in Zoology*, 10, 81.
- Key, M., MacCall, A., Field, J., Aseltin-Nielson, D. & Lynn, K. (2008). *The 2007 assessment of blue rockfish (Sebastes mystinus) in California*. California Department of Fish & Game.
- Komoroske, L.M., Connon, R.E., Jeffries, K.M. & Fanguie, N.A. (2015). Linking transcriptional responses to organismal tolerance reveals mechanisms of thermal sensitivity in a mesothermal endangered fish. *Molecular Ecology*, 24(19), 4960-4981.
- Koweeck, D.A., Nickols, K.J., Leary, P.R., Litvin, S.Y., Bell, T.W., Luthin, T., Lummis, S., Mucciarone, D.A. & Dunbar, R.B. (2017). A year in the life of a central California kelp forest: Physical and biological insights into biogeochemical variability. *Biogeosciences*, 14(1), 31-44.
- Kroeker, K.J., Kordas, R.L., Crim, R.N., & Singh, G.G. (2010). Meta-analysis reveals negative yet variable effects of ocean acidification on marine organisms. *Ecology Letters*, 13(11), 1419-1434.
- Kroeker, K.J., Kordas, R.L., Crim, R., Hendriks, I.E., Ramajo, L., Singh, G.S., Duarte, C.M. & Gattuso, J.P. (2013). Impacts of ocean acidification on marine organisms: Quantifying sensitivities and interaction with warming. *Global Change Biology*, 19(6), 1884-1896.
- Kroeker, K.J., Kordas, R.L. & Harley, C.D.G. (2017). Embracing interactions in ocean acidification research: confronting multiple stressor scenarios and context dependence. *Biology Letters* 13, 20160802.
- Kültz, D. (2005). Molecular and Evolutionary Basis of the Cellular Stress Response. *Annual Review of Physiology*, 67(1), 225-257.
- Langmead, B., Trapnell, C., Pop, M. & Salzberg, S.L. (2009). Ultrafast and memory-efficient alignment of short DNA sequences to the human genome. *Genome Biology*, 10(3), R25.
- Leaman, B. (1991). Reproductive styles and life history variables relative to exploitation and management of *Sebastes* stocks. *Environmental Biology of Fishes*, 30, 253-271.

- Lenarz, W.H., Larson, R.J. & Ralston, S. (1991). Depth distributions of late larvae and pelagic juveniles of some fishes of the California Current. *California Cooperative Oceanic Fisheries Reports*, 32, 41-46.
- Li, B. & Dewey, C.N. (2011). RSEM: Accurate transcript quantification from RNA-Seq data with or without a reference genome. *BMC Bioinformatics*, 12.
- Liu, L. & Simon, M.C. (2004). Regulation of transcription and translation by hypoxia. *Cancer Biology and Therapy*, 3(6), 492-497.
- Liu, Y., Beyer, A. & Aebersold, R. (2016). On the dependency of cellular protein levels on mRNA abundance. *Cell*, 165(3), 535-550.
- Logan, C.A. & Buckley, B.A. (2015). Transcriptomic responses to environmental temperature in eurythermal and stenothermal fishes. *Journal of Experimental Biology*, 218(12), 1915-1924.
- Long, Y., Yan, J., Song, G., Li, X., Li, X., Li, Q. & Cui, Z. (2015). Transcriptional events co-regulated by hypoxia and cold stresses in zebrafish larvae. *BMC Genomics*, 16(1), 1-15.
- Love, M.S., Morris, P. McCrae, M. & Collins, R. (1990). Life history aspects of 19 rockfish species from the Southern California Bight. NOAA Technical Report NMFS 87.
- Love, M.S., Yoklavich, M. & Thorsteinson, L. (2002). *The Rockfishes of the Northeast Pacific*. Berkeley: University of California Press. 405 pp.
- MacManes, M.D. (2014). On the optimal trimming of high-throughput mRNA sequence data. *Frontiers in Genetics*, 5, 1-7.
- Maneja, R.H., Frommel, A.Y., Browman, H.I., Clemmesen, C., Geffen, A.J., Folkvord, A., Piatkowski, U., Durif, C.M.F., Bjelland, R. & Skiftesvik, A.B. (2013). The swimming kinematics of larval Atlantic cod, *Gadus morhua* L., are resilient to elevated seawater $p\text{CO}_2$. *Marine Biology*, 160(8), 1963-1972.
- Mattiasen, E. (6 June 2018). "Effects of hypoxia on the behavior and physiology of juvenile temperate reef fishes (genus: *Sebastes*)." Master of Science Thesis Defense (unpublished), Moss Landing Marine Laboratories, Moss Landing, CA.
- Meire, L., Soetaert, K.E.R. & Meysman, F.J.R. (2013). Impact of global change on coastal oxygen dynamics and risk of hypoxia. *Biogeosciences*, 10(4), 2633-2653.
- Melzner, F., Göbel, S., Langenbuch, M., Gutowska, M.A., Pörtner, H.O. & Lucassen, M. (2009). Swimming performance in Atlantic Cod (*Gadus morhua*) following long-

- term (4-12 months) acclimation to elevated seawater $p\text{CO}_2$. *Aquatic Toxicology*, 92(1), 30-37.
- Melzner, F., Thomsen, J., Koeve, W., Oschlies, A., Gutowska, M.A., Bange, H.W., Hansen, H.P. & Körtzinger, A. (2013). Future ocean acidification will be amplified by hypoxia in coastal habitats. *Marine Biology*, 160(8), 1875-1888.
- Metcalfe, J.D., Le Quesne, W.J.F., Cheung, W.W.L. & Righton, D.A. (2012). Conservation physiology for applied management of marine fish: an overview with perspectives on the role and value of telemetry. *Philosophical Transactions of the Royal Society B*, 367, 1746-1756.
- Mi, H., Muruganujan, A., Ebert, D., Huang, X. & Thomas, P.D. (2019a). PANTHER version 14: more genomes, a new PANTHER GO-slim and improvements in enrichment analysis tools. *Nucleic Acids Research* 47, D419-D426.
- Mi, H., Muruganujan, A., Huang, X., Ebert, D., Mills, C., Guo, X. & Thomas, P.D. (2019b). Protocol Update for large-scale genome and gene function analysis with the PANTHER classification system (v.14.0). *Nature Protocols* 14, 703-721.
- Michael, K., Kreiss, C.M., Hu, M.Y., Koschnick, N., Bickmeyer, U., Dupont, S., Pörtner, H.O. & Lucassen, M. (2016). Adjustments of molecular key components of branchial ion and pH regulation in Atlantic cod (*Gadus morhua*) in response to ocean acidification and warming. *Comparative Biochemistry and Physiology - Part B: Biochemistry and Molecular Biology*, 193, 33-46.
- Michaelidis, B., Spring, A. & Pörtner, H.O. (2007). Effects of long-term acclimation to environmental hypercapnia on extracellular acid-base status and metabolic capacity in Mediterranean fish *Sparus aurata*. *Marine Biology*, 150, 1417-1429.
- Miller, G.M., Watson, S., McCormick, M.I. & Munday, P.L. (2013). Increased CO_2 stimulates reproduction in a coral reef fish. *Global Change Biology*, 19, 3037-3045.
- Miller, S.H., Breitburg, D.L., Burrell, R.B. & Keppel, A.G. (2016). Acidification increases sensitivity to hypoxia in important forage fishes. *Marine Ecology Progress Series*, 549, 1-8.
- Moran, D. & Støttrup, J.G. (2011). The effect of carbon dioxide on growth of juvenile Atlantic cod *Gadus morhua* L. *Aquatic Toxicology*, 102, 24-30.
- Munday, P.L., Crawley, N.E. & Nilsson, G.E. (2009a). Interacting effects of elevated temperature and ocean acidification on the aerobic performance of coral reef fishes. *Marine Ecology Progress Series*, 388, 235-242.
- Munday, P.L., Dixon, D.L., Donelson, J.M., Jones, G.P., Pratchett, M.S., Devitsina, G.V. & Døving, K.B. (2009b). Ocean acidification impairs olfactory discrimination

- and homing ability of a marine fish. *Proceedings of the National Academy of Sciences*, 106(6), 1848-1852.
- Munday, P.L., Dixson, D.L., McCormick, M.I., Meekan, M., Ferrari, M.C.O. & Chivers, D.P. (2010). Replenishment of fish populations is threatened by ocean acidification. *Proceedings of the National Academy of Sciences*, 107(29), 12930-12934.
- Natl. Res. Counc. 2010. *Ocean Acidification: A National Strategy to Meet the Challenges of a Changing Ocean*. Washington, DC: Natl. Res. Counc.
- Natl. Res. Counc. 2011. *Climate Stabilization Targets: Emissions, Concentrations and Impacts over Decades to Millennia*. Washington, DC: Natl. Res. Counc.
- Nilsson, G.E., Dixson, D.L., Domenici, P., McCormick, M.I., Sørensen, C., Watson, S.A. & Munday, P.L. (2012). Near-future carbon dioxide levels alter fish behaviour by interfering with neurotransmitter function. *Nature Climate Change*, 2(3), 201-204.
- Oomen, R.A. & Hutchings, J.A. (2017). Transcriptomic responses to environmental change in fishes: insights from RNA sequencing. *FACETS*, 2, 610-641.
- Orr, J.C., Fabry, V.J., Aumont, O., Bopp, L., Doney, S.C., Feely, R.A., Gnanadesikan, A., Gruber, N., Ishida, A., Joos, F., Key, R.M., Lindsay, K., Maier-Reimer, E., Matear, R., Monfray, P., Mouchet, A., Najjar, R.G., Plattner, G.K., Rodgers, K.B., Sabine, C.L., Sarmiento, J.L., Schlitzer, R., Slater, R.D., Totterdell, I.J., Weirig, M.F., Yamanaka, Y. & Yool, A. (2005). Anthropogenic ocean acidification over the twenty-first century and its impact on calcifying organisms. *Nature*, 437, 681-686.
- Palstra, A.P., Beltran, S., Burgerhout, E., Brittijn, S.A., Magnoni, L.J., Henkel, C.V., Jansen, H.J., van den Thillart, G.E.E.J.M., Spaik, H.P. & Planas, J.V. (2013). Deep RNA sequencing of the skeletal muscle transcriptome in swimming fish. *PLOS ONE*, 8(1), e53171.
- Pierrot, D., Lewis, E. & Wallace, D.W.R. (2006). MS Excel Program Developed for CO₂ System Calculations. ORNL/CDIAC-105a. Carbon Dioxide Information Analysis Center, Oak Ridge National Laboratory, U.S. Department of Energy, Oak Ridge, Tennessee.
- Piggott, J.J., Townsend, C.R. & Matthaei, C.D. (2015). Reconceptualizing synergism and antagonism among multiple stressors. *Ecology and Evolution*, 5(7), 1538-1547.
- Qian, X., Ba, Y., Zhuang, Q. & Zhong, G. (2014). RNA-Seq technology and its application in fish transcriptomics. *OMICS: A Journal of Integrative Biology*, 18(2), 98-110.
- Randall, D. (1982). The control of respiration and circulation in fish during exercise and hypoxia. *Journal of Experimental Biology*, 100, 275-288.

- Richards, J.G. (2009). *Chapter 10: Metabolic and Molecular Responses of Fish to Hypoxia*. In: *Fish Physiology*, 27, 443-485.
- Riebesell, U., Fabry V.J., Hansson, L. & Gattuso, J.P. (Eds.) (2010). Guide to best practices for ocean acidification research and data reporting, 260 p. Luxembourg: Publications Office of the European Union.
- Robinson, M.D., McCarthy, D.J. & Smyth, G.K. (2009). edgeR: A Bioconductor package for differential expression analysis of digital gene expression data. *Bioinformatics*, 26(1), 139-140.
- Schwanhausser, B., Busse, D., Li, N., Dittmar, G., Schuchhardt, J., Wolf, J., Chen, W. & Selbach, M. (2011). Global quantification of mammalian gene expression control. *Nature*, 473, 337-342.
- Simão, F.A., Waterhouse, R.M., Ioannidis, P., Kriventseva, E.V. & Zdobnov, E.M. (2015). BUSCO: Assessing genome assembly and annotation completeness with single-copy orthologs. *Bioinformatics*, 31(19), 3210-3212.
- Simpson, S.D., Munday, P.L., Wittenrich, M.L., Manassa, R., Dixon, D.L., Gagliano, M. & Yan, H.Y. (2011). Ocean acidification erodes crucial auditory behavior in a marine fish. *Biology Letters*, 7(6), 917-920.
- Smith, S., Bernatchez, L. & Beheregaray, L.B. (2013). RNA-seq analysis reveals extensive transcriptional plasticity to temperature stress in a freshwater fish species. *BMC Genomics*, 14, 375.
- Snyder, M.A., Sloan, L.C., Diffenbaugh, N.S. & Bell, J.L. (2003). Future climate change and upwelling in the California Current. *Geophysical Research Letters*, 30(15), 1823.
- Strobel, A., Bennecke, S., Leo, E., Mintenbeck, K., Pörtner, H.O. & Mark, F.C. (2012). Metabolic shifts in the Antarctic fish *Notothenia rossii* in response to rising temperature and $p\text{CO}_2$. *Frontiers in Zoology*, 9, 28.
- Strobel, A., Graeve, M., Pörtner, H.O. & Mark, F.C. (2013a). Mitochondrial acclimation capacities to ocean warming and acidification are limited in the Antarctic nototheniid fish, *Notothenia rossii* and *Lepidonotothen squamifrons*. *PLOS ONE*, 8, e68865.
- Strobel, A., Leo, E., Pörtner, H.O. & Mark, F.C. (2013b). Elevated temperature and $p\text{CO}_2$ shift metabolic pathways in differentially oxidative tissues of *Notothenia rossii*. *Comparative Biochemistry and Physiology - Part B: Biochemistry and Molecular Biology*, 166, 48-57.

- Sydeman, W.J., Garcia-Reyes, M., Schoeman, D.S., Rykaczewski, R.R., Thompson, S.A., Black, B.A. & Bograd, S.J. (2014). Climate change and wind intensification in coastal upwelling ecosystems. *Scientific Reports*, 345(6192), 77-80.
- Terova, G., Rimoldi, S., Corà, S., Bernardini, G., Gornati, R. & Saroglia, M. (2008). Acute and chronic hypoxia affects HIF-1 α mRNA levels in sea bass (*Dicentrarchus labrax*). *Aquaculture*, 279, 150-159.
- Todd, E.V., Black, M.A. & Gemmell, N.J. (2016). The power and promise of RNA-seq in ecology and evolution. *Molecular Ecology*, 25, 1224-1241.
- Ton, C., Stamatiou, D. & Liew, C.C. (2003). Gene expression profile of zebrafish exposed to hypoxia during development. *Physiological Genomics*, 13(2), 97-106.
- Tseng, Y. C., Hu, M. Y., Stumpp, M., Lin, L. Y., Melzner, F., & Hwang, P. P. (2013). CO₂-driven seawater acidification differentially affects development and molecular plasticity along life history of fish (*Oryzias latipes*). *Comparative Biochemistry and Physiology - Part A: Molecular and Integrative Physiology*, 165(2), 1190-1130.
- Val, A.L. (1995). Oxygen transfer in fish: morphological and molecular adjustments. *Brazilian Journal of Medical and Biological Research*, 28, 1119-1127.
- van der Meer, D.L., van den Thillart, G.E.E.J.M., Witte, F., de Bakker, M.A.G., Besser, J., Richardson, M.K., Spaik, H.P., Leito, J.T.D. & Bagowski, C. P. (2005). Gene expression profiling of the long-term adaptive response to hypoxia in the gills of adult zebrafish. *American Journal of Physiology: Regulatory, Integrative & Comparative Physiology*, 289(5), R1512-R1519.
- Vaquer-Sunyer, R. & Duarte, C.M. (2008). Thresholds of hypoxia for marine biodiversity. *Proceedings of the National Academy of Sciences*, 105, 15452-15457.
- Vulesevic, B., McNeill, B. & Perry, S.F. (2006). Chemoreceptor plasticity and respiratory acclimation in the zebrafish *Danio rerio*. *Journal of Experimental Biology*, 209, 1261-1273.
- Wang, Z., Gerstein, M. & Snyder, M. (2009). RNA-Seq: a revolutionary tool for transcriptomics. *Nature Reviews Genetics*, 10, 57-63.
- Warzybok, P., Santora, J.A., Ainley, D.G., Bradley, R.W., Field, J.C., Capitolo, P.J., Carle, R.D., Elliott, M., Beck, J.N., McChesney, G.J., Hester, M.M. & Jahncke, J. (2018). Prey switching and consumption by seabirds in the central California upwelling ecosystem: Implications for forage fish management. *Journal of Marine Systems*, 185, 25-39.

- Wu, R. S. S. (2002). Hypoxia: From molecular responses to ecosystem responses. *Marine Pollution Bulletin*, 45, 35-45.
- Wu, R.S.S. & Woo, N.Y.S. (1985). Respiratory responses and tolerance to hypoxia in two marine teleosts, *Epinephelus akaara* (Temminck and Schlegel) and *Mylio macrocephalus* (Basilewsky). *Hydrobiologia*, 119, 209-217.
- Xiao, W. (2015). The hypoxia signaling pathway and hypoxic adaptation in fishes. *Science China Life Sciences*, 58(2), 148-155.
- Young, J.L., Bornik, Z.B., Marcotte, M.L., Charlie, K.N., Wagner, G.N., Hinch, S.G. & Cooke, S.J. (2006). Integrating physiology and life history to improve fisheries management and conservation. *Fish and Fisheries*, 7, 262-283.

APPENDIX A

SUPPLEMENTARY DATA

Table S1: Weights, standard lengths (SL), and total lengths (TL) of all juvenile blue rockfish individuals examined in the acute time-course.

Fish ID	Treatment	Time-point	Weight (g)	SL (mm)	TL (mm)
Mys13	Control	12h	1.54	46.1	53.2
Mys14	Control	12h	1.71	49.9	56.6
Mys15	Control	12h	2.01	50.7	59.3
Mys16	Control	12h	1.42	46.9	53.5
Mys17	pH 7.6	12h	1.36	46.9	53.4
Mys18	pH 7.6	12h	1.16	42.3	49.8
Mys19	pH 7.6	12h	1.44	45.8	52.1
Mys20	pH 7.6	12h	1.54	46.7	54.3
Mys21	DO 4.0	12h	2.44	50.7	59.2
Mys22	DO 4.0	12h	1.66	48.4	54.6
Mys23	DO 4.0	12h	1.63	49	54.6
Mys24	DO 4.0	12h	2.67	51.2	60.6
7064	Combined	12h	0.89	44.5	51
7065	Combined	12h	1.07	44.6	51.4
7066	Combined	12h	2.04	50.5	57.7
7067	Combined	12h	2.05	50.3	58.2
Mys25	Control	24h	1.96	49.1	58.1
Mys26	Control	24h	1.26	46.7	54
Mys27	Control	24h	1.19	45.1	53.4
Mys28	Control	24h	1.08	45.1	51.2
Mys29	pH 7.6	24h	1.13	44.5	52.4
Mys30	pH 7.6	24h	3.47	60.9	69.5
Mys31	pH 7.6	24h	1.47	49.1	56
Mys32	pH 7.6	24h	1.13	42.2	49.1
Mys33	DO 4.0	24h	1.85	49.9	58.7
Mys34	DO 4.0	24h	1.47	45.5	52.5
Mys35	DO 4.0	24h	0.9	42.9	50.1
Mys36	DO 4.0	24h	1.65	48.2	55.1

Fish ID	Treatment	Time-point	Weight (g)	SL (mm)	TL (mm)
7068	Combined	24h	1.43	46.7	53.5
7069	Combined	24h	1.78	48.5	55
7070	Combined	24h	1.65	47.9	55.7
7071	Combined	24h	1.07	43.1	50.2
Mys49	Control	2wk	1.75	44.2	54.3
Mys50	Control	2wk	1.27	45.9	54.1
Mys51	Control	2wk	1.57	47.2	54.7
Mys52	Control	2wk	1.78	45.8	54.2
Mys53	pH 7.6	2wk	1.72	45.7	54.1
Mys54	pH 7.6	2wk	1.99	50	58.3
Mys55	pH 7.6	2wk	1.38	45.1	52.4
Mys56	pH 7.6	2wk	1.97	48.9	56.8
Mys57	DO 4.0	2wk	1.54	45.9	54.8
Mys58	DO 4.0	2wk	1.6	45.8	55.1
Mys59	DO 4.0	2wk	1.14	44	51.9
Mys60	DO 4.0	2wk	1.65	48	55.5
7076	Combined	2wk	1.51	45.4	54.2
7077	Combined	2wk	1.7	48	56.3
7078	Combined	2wk	2.31	50.3	59.3
7079	Combined	2wk	1.72	49.4	56.6

Table S2: Mean temperature, pH, $p\text{CO}_2$, dissolved inorganic carbon (DIC), total alkalinity (TA), and dissolved oxygen (DO) levels of the four treatments to which blue rockfish were exposed during the two-week time-course.

Treatment	Mean Temp. (°C)	Mean pH	Mean $p\text{CO}_2$ (μatm)	Mean DIC ($\mu\text{mol/kg SW}$)	Total Alkalinity ($\mu\text{mol/kg SW}$)	Mean DO (mg/L)
Control	11.40 (0.11)	8.023 (0.007)	403.8 (6.4)	2042.7 (6.2)	2216.5 (8.8)	8.01 (0.16)
High $p\text{CO}_2$ / low pH	12.03 (0.33)	7.583 (0.017)	1238.9 (56.3)	2208.6 (22.5)	2235.7 (21.9)	8.30 (0.06)
Hypoxic / low DO	12.27 (0.09)	8.02 (0.008)	408.4 (7.3)	2039.8 (5.4)	2217.5 (8.1)	3.93 (0.02)
Cross (high $p\text{CO}_2$ / low DO)	11.58 (0.34)	7.595 (0.027)	1194.5 (91.8)	2192.5 (44.7)	2221.3 (41.7)	3.92 (0.04)

Table S3: Eleven blue rockfish tissue samples from which mRNA was isolated, cDNA libraries were constructed, Illumina[®] sequence information was generated and a *de novo* transcriptome was created. All libraries were paired-end (PE) except the three marked with asterisks (*), which were single-end (SE) libraries sourced from the experimental time-course.

Fish ID	Treatment	Time-point	Tissue
Mys_0_B	Control	0 h	brain
Mys_0_L	Control	0 h	liver
7069	Combined	24 h	gill
Mys161	DO 4.0	6 mo	gill
Mys259	pH 7.5	6 mo	gill
7068	Combined	24 h	muscle
Mys165	DO 4.0	6 mo	muscle
Mys252	pH 7.5	6 mo	muscle
Mys53*	pH 7.5	2 wk	muscle
Mys57*	DO 4.0	2 wk	muscle
7076*	Combined	2 wk	muscle

Table S4: Mean read sizes and read totals before and after Trimmomatic QC trimming and filtering of all paired-end (PE) and single-end (SE) sequence files used to construct the blue rockfish *de novo* transcriptome and perform the differential gene expression analysis. Statistics for the paired-end (PE) reads apply to both the forward (R1) and reverse (R2) reads that were paired after trimming and incorporated into the *de novo* assembly (Trinity does not incorporate PE reads that are unpaired after trimming).

Fish/File ID	Treatment	Time-point	Pre-QC		Post-QC	
			Mean Read Size (bp)	Total # PE Reads	Mean Read Size (bp)	Total # PE Reads
<i>De novo</i>				398,410,942		235,975,049
Mys_0_B	Control	0h	151	55,620,582	150.98	32,551,698
Mys_0_L	Control	0h	151	66,257,155	150.98	42,382,445
Mys252	pH 7.5	6mo	151	37,180,620	150.98	20,103,887
Mys259	pH 7.5	6mo	151	58,493,852	150.98	32,192,367
Mys161	DO 4.0	6mo	151	39,461,465	150.98	27,841,021
Mys165	DO 4.0	6mo	151	47,075,883	150.98	34,194,227
7068	Cross	24h	151	44,779,488	150.98	22,876,866
7069	Cross	24h	151	49,541,897	150.98	23,832,538

Fish/File ID	Treatment	Time-point	Pre-QC		Post-QC	
			Mean Read Size (bp)	Total # SE Reads	Mean Read Size (bp)	Total # SE Reads
<i>Time-course</i>				776,060,318		771,166,351
Mys13	Control	12h	51	12,727,920	50.98	12,713,785
Mys14	Control	12h	51	17,630,260	50.99	17,618,520
Mys15	Control	12h	51	13,783,923	50.98	13,043,267
Mys16	Control	12h	51	13,449,926	50.98	13,426,336
Mys17	pH 7.5	12h	51	19,340,677	50.98	19,047,919
Mys18	pH 7.5	12h	51	19,349,035	50.98	19,013,334
Mys19	pH 7.5	12h	51	38,169,202	50.98	38,138,073
Mys20	pH 7.5	12h	51	18,113,019	50.98	18,101,246
Mys21	DO 4.0	12h	51	17,634,252	50.98	17,613,183
Mys22	DO 4.0	12h	51	26,234,935	50.98	26,082,503
Mys23	DO 4.0	12h	51	14,378,646	50.99	14,352,716
Mys24	DO 4.0	12h	51	14,579,059	50.98	14,386,966
7064	Cross	12h	51	32,267,458	50.98	31,662,789
7065	Cross	12h	51	35,981,427	50.98	35,798,493
7066	Cross	12h	51	19,693,491	50.99	19,683,192
7067	Cross	12h	51	11,388,832	50.99	11,384,555
Mys25	Control	24h	51	24,802,340	50.98	24,609,193
Mys26	Control	24h	51	15,798,612	50.98	15,767,321
Mys27	Control	24h	51	14,670,899	50.98	14,616,365
Mys28	Control	24h	51	10,297,933	50.99	10,257,254
Mys30	pH 7.5	24h	51	15,747,852	50.98	15,635,227
Mys31	pH 7.5	24h	51	17,416,433	50.98	17,388,883
Mys32	pH 7.5	24h	51	18,587,147	50.98	18,545,501
Mys34	DO 4.0	24h	51	18,175,850	50.98	17,701,625
Mys35	DO 4.0	24h	51	20,367,295	50.98	20,354,053
Mys36	DO 4.0	24h	51	14,832,363	50.99	14,816,428

Fish/File ID	Treatment	Time-point	Mean Read Size (bp)	Total # SE Reads	Mean Read Size (bp)	Total # SE Reads
7068	Cross	24h	51	15,144,745	50.98	15,131,662
7069	Cross	24h	51	15,196,808	50.98	15,133,676
7070	Cross	24h	51	14,951,744	50.98	14,923,514
7071	Cross	24h	51	13,435,403	50.99	13,412,936
Mys49	Control	2wk	51	13,440,498	50.98	13,360,606
Mys50	Control	2wk	51	16,357,180	50.97	16,130,310
Mys51	Control	2wk	51	16,229,708	50.99	16,217,789
Mys52	Control	2wk	51	18,614,315	50.98	18,600,238
Mys53	pH 7.5	2wk	51	12,931,448	50.98	12,797,362
Mys54	pH 7.5	2wk	51	13,809,824	50.98	13,761,457
Mys57	DO 4.0	2wk	51	15,519,207	50.97	15,449,294
Mys58	DO 4.0	2wk	51	17,692,314	50.98	17,403,940
Mys59	DO 4.0	2wk	51	15,865,426	50.98	15,850,225
Mys60	DO 4.0	2wk	51	15,694,820	50.99	15,677,482
7076	Cross	2wk	51	17,348,220	50.98	17,228,807
7077	Cross	2wk	51	11,306,869	50.99	11,293,989
7078	Cross	2wk	51	18,820,794	50.98	18,790,475
7079	Cross	2wk	51	18,282,209	50.99	18,243,862

Table S5: 293 blue rockfish muscle tissue genes that were differentially expressed between a control treatment and high $p\text{CO}_2$, hypoxic and combined high $p\text{CO}_2$ /hypoxic treatments. Genes were successfully annotated against the UniProt/SwissProt sequence database. In the Significant Pairwise Comparison columns, the “U” and “D” designations respectively indicate up-regulation and down-regulation at 12 h, 24 h, and/or two weeks in either the high $p\text{CO}_2$ (1-3), hypoxic (4-6), or combined stressor (7-9) treatments.

UniProtKB ID	Category	UniProt Gene Name	Min. E-value	Significant Pairwise Comparison
P10286	Activity, hormonal	Calcitonin gene-related peptide	4.20E-50	8U
Q29437	Amine oxidase	Primary amine oxidase, liver isozyme	1.40E-180	8U
Q8K1S5	Apoptosis	Krueppel-like factor 11	3.00E-51	4D
Q5SPB6	Apoptosis	Glutathione-specific gamma-glutamylcyclotransferase 1	2.10E-79	4D
O55003	Apoptosis	BCL2/adenovirus E1B 19 kDa protein-interacting protein 3	6.60E-48	8D
P27469	Apoptosis	G0/G1 switch protein 2	8.60E-08	8U
Q36964	ATP synthesis	ATP synthase subunit a	5.90E-22	1D 2U 5U
P56381	ATP synthesis	ATP synthase subunit epsilon, mitochondrial	2.40E-09	3U
Q14964	Autophagy	Ras-related protein Rab-39A	2.30E-58	4D
Q9Y4G2	Autophagy	Pleckstrin homology domain-containing family M member 1	3.50E-240	4D
Q6GMH3	Binding, actin	Twinfilin-2	3.80E-159	8D
Q56A55	Binding, ATP	ATP-binding cassette sub-family B member 8, mitochondrial	9.20E-302	4D
Q6AXL4	Binding, calcium	Neurocalcin-delta B	1.80E-104	8U
A2BGD5	Binding, calcium	Calcium-binding and coiled-coil domain-containing protein 1	2.10E-56	8D
Q6PJW8	Binding, connexin	Consortin	1.70E-06	8D
P62803	Binding, DNA	Histone H4	4.50E-51	8D
Q4R8G6	Binding, DNA	Meiosis-specific with OB domain-containing protein	8.40E-142	8U
P84227	Binding, DNA	Histone H3.2	9.30E-67	5D
Q9Z180	Binding, DNA	SET-binding protein	7.60E-151	8U
Q8BG87	Binding, DNA	Methylcytosine dioxygenase TET3	4.50E-271	8U
Q80SU7	Binding, GTP	Interferon-induced very large GTPase 1	6.70E-47	1D 8U
Q7Z2Y8	Binding, GTP	Interferon-induced very large GTPase 1	9.40E-45	8U
B6D985	Binding, hemoglobin	Haptoglobin	1.80E-39	8D
Q09139	Binding, lipid	Fatty acid-binding protein, brain	7.20E-55	3U
P49946	Binding, metal ion	Ferritin, heavy subunit	9.80E-27	4D

UniProtKB ID	Category	UniProt Gene Name	Min. E-value	Significant Pairwise Comparison		
Q400C8	Binding, metal ion	Archaemetzincin-2	1.20E-120	4U		
P40148	Binding, metal ion	Osteocalcin	6.60E-36	8U		
O42430	Binding, metal ion	Cytochrome P450 1A1	1.80E-278	8U		
P78325	Binding, metal ion	Disintegrin and metalloproteinase domain-containing protein 8	8.60E-147	8D		
Q0I159	Binding, metal ion	Pyridoxal kinase	9.10E-129	8U		
P47875	Binding, metal ion	Cysteine and glycine-rich protein 1	2.70E-95	5U		
Q5ZHN5	Binding, metal ion	THAP domain-containing protein 5	3.80E-23	8D		
P52727	Binding, metal ion	Metallothionein A	6.50E-09	3U	6U	
Q9P2E3	Binding, metal ion	NFX1-type zinc finger-containing protein 1	0.00E+00	3D		
Q7ZUP1	Binding, RNA	Terminal nucleotidyltransferase 5C	4.40E-186	8U		
Q06AT9	Binding, RNA	RNA-binding protein 4B	1.80E-49	6D		
Q8SQ27	Binding, RNA	RNA-binding protein 12	1.60E-154	6D		
Q92823	Cell adhesion	Neuronal cell adhesion molecule	0.00E+00	8U		
P40239	Cell adhesion	CD9 antigen	2.70E-58	8U		
Q14112	Cell adhesion	Nidogen-2	1.40E-191	8U		
Q7Z7G0	Cell adhesion	Target of Nesh-SH3	2.00E-121	3U		
Q61824	Cell adhesion	Disintegrin and metalloproteinase domain-containing protein 12	9.90E-269	3D		
Q9UJX6	Cell cycle	Anaphase-promoting complex subunit 2	7.70E-229	8U		
Q8NDN9	Cell cycle	RCC1 and BTB domain-containing protein 1	1.10E-06	8D		
Q6GM07	Cell cycle	Cyclin-dependent kinase 2-interacting protein	4.60E-39	3U		
O08665	Cell differentiation	Semaphorin-3A	2.40E-252	3D		
P41987	Cell-cell adhesion	Gap junction alpha-3 protein	5.40E-97	4D		
Q08DQ0	Cell-cell adhesion	Plakophilin-3	7.30E-168	6D		
O75712	Cell-cell adhesion	Gap junction beta-3 protein	4.30E-97	3U		
P28827	Cell-cell adhesion	Receptor-type tyrosine-protein phosphatase mu	0.00E+00	3U		
Q96CD2	Coenzyme A synthesis	Phosphopantothencysteine decarboxylase	3.40E-78	8D		
P79331	Collagen degradation	A disintegrin and metalloproteinase with thrombospondin motifs 2	2.60E-293	3U		
Q8R5F7	Defense response to virus	Interferon-induced helicase C domain-containing protein 1	3.70E-243	3D		
P11247	Defense response to microbes	Myeloperoxidase	8.90E-164	8U		
Q53G44	Defense response to virus	Interferon-induced protein 44-like	1.10E-42	3D		
Q6P8X6	Deubiquitination	Putative ubiquitin carboxyl-terminal hydrolase 50	5.10E-14	8U		
Q4R6D3	Deubiquitination	Putative ubiquitin carboxyl-terminal hydrolase 50	3.60E-06	8U		
P34810	Endosome/Lysosome	Macrosialin	5.40E-16	3D		

UniProtKB ID	Category	UniProt Gene Name	Min. E-value	Significant Pairwise Comparison
P04233	Immune response	HLA class II histocompatibility antigen gamma chain	1.80E-20	8U
P20755	Immune response	RLA class II histocompatibility antigen, DP alpha-1 chain	3.60E-06	8U
Q4JQ11	Metabolism, aerobic	Cytochrome c oxidase subunit 3	9.10E-30	2U 3U 4U 5U 6U
Q36775	Metabolism, aerobic	Cytochrome c oxidase subunit 1	3.70E-33	8U
Q945D0	Metabolism, aerobic	Cytochrome b	2.20E-31	3U
Q37741	Metabolism, aerobic	Cytochrome c oxidase subunit 2	2.20E-37	3D
Q5RC24	Metabolism, aerobic	Cytochrome b-c1 complex subunit 7	2.90E-42	3U
Q8SGA0	Metabolism, aerobic	Cytochrome b	5.30E-25	9U
P80971	Metabolism, aerobic	Cytochrome c oxidase subunit 4 isoform 2, mitochondrial	8.80E-67	3U
P05123	Metabolism, amino acid	Creatine kinase M-type	2.80E-53	1U 3U 3D 4U 5U 6D 8U
P54886	Metabolism, amino acid	Delta-1-pyrroline-5-carboxylate synthase	0.00E+00	6U
Q5R9C1	Metabolism, carbohydrate	6-phosphofructo-2-kinase/fructose-2,6-bisphosphatase 3	1.30E-225	4D
P25114	Metabolism, carbohydrate	6-phosphofructo-2-kinase/fructose-2,6-bisphosphatase 4	5.00E-233	2U
Q16877	Metabolism, carbohydrate	6-phosphofructo-2-kinase/fructose-2,6-bisphosphatase 4	9.40E-196	8D
Q9P2W7	Metabolism, carbohydrate	Galactosylgalactosylxylosylprotein 3-beta-glucuronosyltransferase 1	1.00E-170	8U
Q5X110	Metabolism, carbohydrate - glycolysis	Glyceraldehyde-3-phosphate dehydrogenase	7.90E-30	2U 8U
B5DGM7	Metabolism, carbohydrate - glycolysis	Fructose-bisphosphate aldolase A	1.60E-174	6U 8U 9U
Q5MJ86	Metabolism, carbohydrate - glycolysis	Glyceraldehyde-3-phosphate dehydrogenase 2	3.40E-179	8U
Q0P4F7	Metabolism, lipid	Acyl-CoA synthetase family member 2, mitochondrial	1.90E-245	1U 4U
Q99P15	Metabolism, lipid	Phosphatidate phosphatase LPIN2	2.00E-199	4D
Q924N5	Metabolism, lipid	Long-chain-fatty-acid--CoA ligase ACSBG1	1.10E-250	7U
Q8BJ56	Metabolism, lipid	Patatin-like phospholipase domain-containing protein 2	5.00E-158	4D
Q92539	Metabolism, lipid	Phosphatidate phosphatase LPIN2	5.90E-216	8D
Q0VD19	Metabolism, lipid	Sphingomyelin phosphodiesterase	2.70E-190	8D
A2VE15	Metabolism, lipid	Fatty acid desaturase 6	6.60E-117	6D
Q9NZ01	Metabolism, lipid	Very-long-chain enoyl-CoA reductase	7.40E-138	6U
Q8VCC1	Metabolism, lipid	15-hydroxyprostaglandin dehydrogenase	7.40E-83	3U
P11602	Metabolism, lipid	Lipoprotein lipase	3.40E-90	3D
P41320	Metabolism, nitrogen	Glutamine synthetase, mitochondrial	2.40E-202	4D 8D
Q01432	Metabolism, nucleoside	AMP deaminase 3	3.90E-277	8D

UniProtKB ID	Category	UniProt Gene Name	Min. E-value	Significant Pairwise Comparison	
P85281	Metabolism, nucleoside	Nucleoside diphosphate kinase B	1.20E-21	4U	
A3KFX0	Metabolism, nucleoside	Cytosolic 5'-nucleotidase 1A	7.60E-143	3U	
P12115	Metabolism, nucleoside	Adenylate kinase isoenzyme 1	3.40E-27	3U	
Q91YD3	mRNA decapping	mRNA-decapping enzyme 1A	7.50E-79	8D	
P68246	Muscle contraction	Troponin I, fast skeletal muscle	2.20E-32	4D	5D
P70083	Muscle contraction	Sarcoplasmic/endoplasmic reticulum calcium ATPase 1	1.40E-22	1U	3U 5U 9U
Q90339	Muscle contraction	Myosin heavy chain, fast skeletal muscle	7.20E-156	2U	3U
P02562	Muscle contraction	Myosin heavy chain, skeletal muscle	5.80E-24	2U	
Q9WUZ5	Muscle contraction	Troponin I, slow skeletal muscle	3.00E-53	2U	5U
P50751	Muscle contraction	Troponin T, cardiac muscle	7.80E-36	2U	
P04460	Muscle contraction	Myosin-6	5.90E-19	2U	
P02609	Muscle contraction	Myosin regulatory light chain 2, skeletal muscle isoform	2.30E-12	3U	
P82159	Muscle contraction	Myosin light chain 1, skeletal muscle isoform	1.80E-36	3U	
P97457	Muscle contraction	Myosin regulatory light chain 2, skeletal muscle isoform	6.40E-20	3U	
Q076A3	Muscle contraction	Myosin-13	4.60E-26	3U	
Q05AX4	NA	Musculoskeletal embryonic nuclear protein 1	4.20E-15	4D	
Q1LYM6	NA	Kelch-like protein 38	5.50E-239	4D	
Q8N394	NA	Transmembrane and TPR repeat-containing protein 2	2.90E-259	4D	
Q9NZH0	NA	G-protein coupled receptor family C group 5 member B	9.50E-97	8U	
Q2KUJ3	NA	Protein FAM49B	7.70E-141	8U	
Q9BYL1	NA	Sterile alpha motif domain-containing protein 10	2.50E-50	8U	
Q8TGM7	NA	Putative uncharacterized protein ART2	4.10E-14	2U	5U
Q0VF94	NA	NTPase KAP family P-loop domain-containing protein 1	3.60E-74	2D	
Q68CR1	NA	Protein sel-1 homolog 3	1.10E-157	8D	
O42596	NA	Disintegrin and metalloproteinase domain-containing protein 22	0.00E+00	8U	
A2RUH7	NA	Myosin-binding protein H-like	3.90E-13	3U	
Q3UUV48	NA	Leucine-rich repeat-containing protein 30	2.10E-07	6D	
Q8CDN9	NA	Leucine-rich repeat-containing protein 9	1.30E-249	6U	
Q96L08	NA	Sushi domain-containing protein 3	3.20E-22	3U	
Q2WVGJ9	NA	Fer-1-like protein 6	0.00E+00	6U	
Q6PBP3	Oxidation-reduction	Peroxisome-like 2A	3.70E-68	8U	
Q8JFV8	Oxidoreductase	Synaptic vesicle membrane protein VAT-1 homolog	2.10E-180	8U	
Q90YCO	Protein synthesis	Elongation factor 1-gamma	1.40E-42	5D	8D

UniProtKB ID	Category	UniProt Gene Name	Min. E-value	Significant Pairwise Comparison	
Q9H8H1	Protein synthesis	Peptide deformylase, mitochondrial	6.80E-15	3U	
Q26636	Proteolysis	Cathepsin L	3.20E-103	1U	
P35031	Proteolysis	Trypsin-1	4.60E-120	6D	
Q5EB28	Proteolysis	Midnolin	8.70E-56	8D	
Q3T112	Proteolysis	Proteasome subunit beta type-8	3.70E-103	8U	
Q02038	Proteolysis	Neurolysin, mitochondrial	2.50E-249	8D	
Q14520	Proteolysis	Hyaluronan-binding protein 2	2.70E-115	3U	
O75844	Proteolysis	CAAX prenyl protease 1 homolog	4.30E-219	3U	
Q76176	Regulation, cytoskeletal	Protein phosphatase Slingshot homolog 2	2.70E-231	2D	5D
P47805	Regulation, cytoskeletal	Mid1-interacting protein 1A	2.40E-15	4D	8D
P02640	Regulation, cytoskeletal	Villin-1	2.30E-275	4D	
Q8C8H8	Regulation, cytoskeletal	Kyphoscoliosis peptidase	3.10E-54	8D	
P11137	Regulation, cytoskeletal	Microtubule-associated protein 2	3.10E-10	8D	
Q16643	Regulation, cytoskeletal	Drebrin	3.70E-84	8U	
Q6PER3	Regulation, cytoskeletal	Microtubule-associated protein RP/EB family member 3	2.10E-27	8D	
Q9UIW2	Regulation, cytoskeletal	Plexin-A1	0.00E+00	8U	
Q5PQP4	Regulation, cytoskeletal	Cdc42 effector protein 2	3.80E-23	8D	
Q12955	Regulation, cytoskeletal	Ankyrin-3	1.60E-61	3U	
P30427	Regulation, cytoskeletal	Plectin	0.00E+00	3D	
Q86UU1	Regulation, cytoskeletal	Plectstrin homology-like domain family B member 1	8.20E-17	3D	
O43157	Regulation, cytoskeletal	Plexin-B1	1.70E-128	3D	
Q96KS0	Regulation, HIF	Egln9 homolog 2	1.70E-107	8U	
Q7T163	Regulation, protein kinase	Kinase D-interacting substrate of 220 kDa B	6.20E-08	4D	
P28652	Regulation, protein kinase	Calcium/calmodulin-dependent protein kinase type II subunit beta	1.70E-08	4U	
Q924C5	Regulation, protein kinase	Alpha-protein kinase 3	9.20E-57	4D	
O70405	Regulation, protein kinase	Serine/threonine-protein kinase ULK1	1.00E-217	8D	
Q80ZW0	Regulation, protein kinase	Serine/threonine-protein kinase 35	1.40E-164	4D	
Q77PK6	Regulation, protein kinase	Serine/threonine-protein kinase WNK4	5.70E-130	8D	
Q8IY84	Regulation, protein kinase	Serine/threonine-protein kinase NIM1	1.30E-127	4D	8D
Q504Y2	Regulation, protein kinase	Extracellular tyrosine-protein kinase PKDCC	1.10E-110	4U	
Q9WVC7	Regulation, protein kinase	A-kinase anchor protein 6	1.90E-246	8U	
Q15349	Regulation, protein kinase	Ribosomal protein S6 kinase alpha-2	0.00E+00	8D	
Q7L7X3	Regulation, protein kinase	Serine/threonine-protein kinase TAO1	9.60E-17	2D	

UniProtKB ID	Category	UniProt Gene Name	Min. E-value	Significant Pairwise Comparison	
B1WBU5	Regulation, protein kinase	Serine/threonine-protein kinase SBK2	1.30E-54	9U	
Q9DGE0	Regulation, protein kinase	Dual specificity mitogen-activated protein kinase 6	1.80E-177	3D	
Q9D119	Regulation, protein phosphatase	Protein phosphatase 1 regulatory subunit 27	1.60E-50	8D	
P83456	Regulation, protein phosphatase	Alkaline phosphatase	2.10E-242	8U	
Q5SWA1	Regulation, translation	Protein phosphatase 1 regulatory subunit 15B	9.70E-07	8D	
Q66HV7	Regulation, translation	Eukaryotic translation initiation factor 4E type 3	1.30E-66	8D	
Q1LXK5	Regulation, translation	Putative helicase mov-10-B.2	9.90E-295	3D	
Q20A00	Response to DNA damage	DNA damage-inducible transcript 4-like protein	1.50E-45	8D	
P56581	Response to DNA damage	G/T mismatch-specific thymine DNA glycosylase	1.20E-13	8D	
Q14159	Response to DNA damage	DNA repair-scaffolding protein	2.00E-115	8D	
Q2KIX1	Response to DNA damage	Growth arrest and DNA damage-inducible protein GADD45 gamma	8.40E-55	3U	
O75771	Response to DNA damage	DNA repair protein RAD51 homolog 4	4.90E-83	3D	
Q8IVG5	Signaling	Sterile alpha motif domain-containing protein 9-like	1.90E-149	1D	6D
Q68D51	Signaling	DENN domain-containing protein 2C	3.10E-209	4D	
P81122	Signaling	Insulin receptor substrate 2	1.50E-240	4D	8D
Q69Z37	Signaling	Sterile alpha motif domain-containing protein 9-like	4.40E-16	1D	
P58003	Signaling	Sestrin-1	9.90E-216	4D	
Q5K651	Signaling	Sterile alpha motif domain-containing protein 9	7.20E-07	1D	
P19941	Signaling	Growth hormone receptor	1.10E-77	4D	
Q9D684	Signaling	Ras and Rab interactor 2	9.00E-54	4D	
P82951	Signaling	Hepcidin	1.60E-19	8D	
O95490	Signaling	Adhesion G protein-coupled receptor L2	1.90E-65	4D	
O88667	Signaling	GTP-binding protein RAD	8.60E-102	8D	
P07700	Signaling	Beta-1 adrenergic receptor	1.10E-117	8U	
Q13322	Signaling	Growth factor receptor-bound protein 10	2.70E-11	8D	
O62657	Signaling	Stromal cell-derived factor 1	1.80E-14	3D	8U
Q6P3K7	Signaling	Casein kinase I isoform delta-B	2.00E-209	8U	
Q99JZ7	Signaling	ERBB receptor feedback inhibitor 1	3.00E-28	3U	
P50228	Signaling	C-X-C motif chemokine 5	3.80E-09	6U	
Q5DU56	Signaling	Protein NLRC3	4.60E-09	9D	
Q29627	Signaling	Pituitary adenylate cyclase-activating polypeptide type I receptor	6.90E-206	3D	
Q9NZJ4	Stress response, molecular chaperone	Sacsin	0.00E+00	3D	

UniProtKB ID	Category	UniProt Gene Name	Min. E-value	Significant Pairwise Comparison
O35162	Stress response, molecular chaperone	Heat shock 70 kDa protein 13	3.70E-172	9D
Q03692	Structural, collagen	Collagen alpha-1 chain	5.50E-46	1U
Q3U962	Structural, collagen	Collagen alpha-2 chain	4.30E-89	6D
P15988	Structural, collagen	Collagen alpha-2 chain	3.60E-114	8U
P02457	Structural, collagen	Collagen alpha-1	9.80E-105	6D 8U
Q02788	Structural, collagen	Collagen alpha-2 chain	1.70E-48	8U
P13944	Structural, collagen	Collagen alpha-1	0.00E+00	6D
Q61245	Structural, collagen	Collagen alpha-1 chain	4.30E-139	6D
P02460	Structural, collagen	Collagen alpha-1	1.30E-34	6D
P18520	Structural, cytoskeletal	Intermediate filament protein ON3	7.50E-39	8U
P28661	Structural, cytoskeletal	Septin-4	3.50E-78	2D 4D 8D
Q5R8S9	Structural, cytoskeletal	Keratin, type I cytoskeletal 19	1.40E-104	8U
Q8BML1	Structural, cytoskeletal	[F-actin]-monooxygenase MICAL2	0.00E+00	8D
P27130	Structural, cytoskeletal	Actin, muscle 2/4/4A	2.80E-35	3U
P08537	Structural, microtubule	Tubulin alpha chain	1.20E-18	4D
P15146	Structural, microtubule	Microtubule-associated protein 2	2.00E-23	2D 4D
P24634	Structural, microtubule	Tubulin alpha-2 chain	9.20E-78	2D
O57592	Structural, ribosomal	60S ribosomal protein L7a	3.40E-37	1D 3U 4D 8U
Q3T057	Structural, ribosomal	60S ribosomal protein L23	1.40E-14	1U 3U 3D 8D
Q9NFK5	Structural, ribosomal	39S ribosomal protein L39, mitochondrial	2.10E-13	4U
Q90YW0	Structural, ribosomal	60S ribosomal protein L9	4.40E-20	1U 4U
Q56JX8	Structural, ribosomal	40S ribosomal protein S13	3.00E-29	8U
Q7ZY51	Structural, ribosomal	60S ribosomal protein L19	1.50E-21	3U
Q4QY71	Structural, ribosomal	40S ribosomal protein SA	2.50E-36	3U 9D
Q3SZ90	Structural, ribosomal	60S ribosomal protein L13a	2.40E-33	3U
P61155	Structural, ribosomal	40S ribosomal protein S19	3.70E-10	3U
Q9DFQ7	Structural, ribosomal	60S ribosomal protein L24	3.70E-07	3U
P15126	Structural, ribosomal	60S ribosomal protein L5-B	1.90E-26	3D
Q90YT6	Structural, ribosomal	60S ribosomal protein L32	1.80E-17	3U
P42899	Structural, ribosomal	60S acidic ribosomal protein P2	2.00E-13	3U
P58372	Structural, ribosomal	60S ribosomal protein L30	2.80E-32	3U
Q90Z10	Structural, ribosomal	60S ribosomal protein L13	2.60E-32	3U

UniProtKB ID	Category	UniProt Gene Name	Min. E-value	Significant Pairwise Comparison	
				2U	3D
Q8WZ42	Structural, sarcomere	Titin	0.00E+00	2U	3D
A2ASS6	Structural, sarcomere	Titin	1.30E-178	2U	3D
Q5VST9	Structural, sarcomere	Obscurin	2.10E-272	3D	
Q86RN8	Structural, sarcomere	Paramyosin	1.30E-10	3U	
P20929	Structural, sarcomere	Nebulin	7.90E-90	3U	
Q91453	Toxins	Stonustoxin subunit beta	7.30E-21	7U	
Q98989	Toxins	Stonustoxin subunit alpha	2.50E-17	8D	
P18847	Transcription	Cyclic AMP-dependent transcription factor ATF-3	1.70E-38	4D	
O93375	Transcription	Transcription factor COE2	9.70E-129	3U	
Q8AW52	Transcription	Protein atonal homolog 7	4.20E-40	4D	
Q00322	Transcription	CCAAT/enhancer-binding protein delta	8.60E-26	4D	
P81269	Transcription	Cyclic AMP-dependent transcription factor ATF-1	7.70E-23	4D	8D
Q5FVB2	Transcription	LIM domain transcription factor LMO4.1	6.40E-74	4D	6D
Q6IRB2	Transcription	Transcription factor HES-1-A	6.20E-75	4D	
Q5ZL67	Transcription	Endoplasmic reticulum membrane sensor NFE2L1	8.30E-76	8D	
O35185	Transcription	Class E basic helix-loop-helix protein 40	3.00E-115	4D	
Q6IMZ0	Transcription	Nuclear factor interleukin-3-regulated protein	2.00E-14	4D	
P55199	Transcription	RNA polymerase II elongation factor ELL	3.70E-119	8D	
O95931	Transcription	Chromobox protein homolog 7	1.70E-33	4D	
Q2LE08	Transcription	Forkhead box protein P1-B	1.20E-102	4D	8D
Q96BF6	Transcription	Nucleus accumbens-associated protein 2	3.60E-135	5U	
Q06413	Transcription	Myocyte-specific enhancer factor 2C	2.00E-13	8D	
Q4R6W9	Transcription	snRNA-activating protein complex subunit 1	1.70E-59	8D	
Q9HCM3	Transcription	UPF0606 protein KIAA1549	1.30E-197	8U	
Q9ULV5	Transcription	Heat shock factor protein 4	1.60E-71	8D	
Q1RMRO	Transcription	DNA-directed RNA polymerase III subunit RPC7-like	6.20E-07	3U	
Q3KNV8	Transcription	Polycomb group RING finger protein 3	3.70E-126	3U	
O88712	Transcription	C-terminal-binding protein 1	1.50E-149	6D	
Q1KL16	Transcription	Homeobox protein Hox-A10a	1.30E-76	6D	
Q5M7V8	Transcription	Thyroid hormone receptor-associated protein 3	1.50E-47	6D	
Q1KKV2	Transcription	Homeobox protein Hox-C11a	3.40E-111	6D	
Q1KKU7	Transcription	Homeobox protein Hox-C5a	1.20E-69	6U	
Q1KL17	Transcription	Homeobox protein Hox-A11a	7.30E-86	6D	

UniProtKB ID	Category	UniProt Gene Name	Min. E-value	Significant Pairwise Comparison		
				2D	4D	8D
A5D7T4	Transferase	Beta-galactoside alpha-2,6-sialyltransferase 2	1.10E-118	2D	4D	8D
P13913	Transferase	Arylamine N-acetyltransferase, pineal gland isozyme NAT-10	1.60E-85	8U		
Q5RDU4	Transferase	Poly [ADP-ribose] polymerase 6	1.40E-232	6U		
P51143	Transport, amine	Sodium-dependent noradrenaline transporter	8.30E-277	8U		
Q5HZE0	Transport, amino acid	Mitochondrial basic amino acids transporter	1.10E-11	4U		
Q7YQK3	Transport, amino acid	4F2 cell-surface antigen heavy chain	4.10E-112	4D	8D	
A1L1W9	Transport, amino acid	Monocarboxylate transporter 10	1.80E-211	4D		
Q503G8	Transport, amino acid	Probable sodium-coupled neutral amino acid transporter 6	1.10E-112	8D		
Q9UN76	Transport, amino acid	Sodium- and chloride-dependent neutral and basic amino acid transporter B	4.50E-222	5U		
P83299	Transport, bicarbonate	Carbonic anhydrase 1	1.2E-259	4U		
Q92051	Transport, bicarbonate	Carbonic anhydrase	1.70E-130	9U		
Q5R1P0	Transport, ion	Glutamate receptor ionotropic, NMDA 1	2.90E-116	4D	8D	
P70406	Transport, ion	Mitochondrial uncoupling protein 2	6.80E-132	4D		
O15247	Transport, ion	Chloride intracellular channel protein 2	1.20E-100	8U		
P14415	Transport, ion	Sodium/potassium-transporting ATPase subunit beta-2	2.50E-95	5U		
Q8TDI7	Transport, ion	Transmembrane channel-like protein 2	4.60E-93	8D		
Q9YH26	Transport, ion	Sodium/potassium-transporting ATPase subunit alpha-1	6.80E-86	8U		
Q8TDI8	Transport, ion	Transmembrane channel-like protein 1	9.40E-129	8D		
P58312	Transport, ion	Sodium/potassium-transporting ATPase subunit alpha-3	1.10E-202	8U		
P01131	Transport, lipid	Low-density lipoprotein receptor	1.10E-167	4D		
Q45KW7	Transport, lipid	Fatty acid-binding protein, intestinal	1.20E-48	3U	6U	
Q28BP2	Transport, membrane	Transmembrane protein 150A	6.60E-113	4U	6D	8U 9D
P84653	Transport, oxygen	Hemoglobin subunit alpha-1	2.30E-20	2U		
Q9PVU6	Transport, oxygen	Hemoglobin embryonic subunit alpha	4.00E-60	9U		
P83273	Transport, oxygen	Hemoglobin subunit beta-2	7.00E-35	6U	9U	
Q8CB87	Transport, protein	Ras-related protein Rab-44	2.20E-37	4D		
Q17QB7	Transport, protein	Ras-related protein Rab-30	1.10E-73	5U		
Q8N4G2	Transport, protein	ADP-ribosylation factor-like protein 14	1.20E-47	3U		
Q8C437	Transport, protein	PEX5-related protein	5.90E-121	6U		
Q14258	Ubiquitination	E3 ubiquitin/ISG15 ligase TRIM25	1.20E-33	4D		
Q91Z63	Ubiquitination	E3 ubiquitin-protein ligase TRIM63	1.50E-99	4D	8D	
Q9PW70	Ubiquitination	Cytokine-inducible SH2-containing protein	3.10E-41	4D		

UniProtKB ID	Category	UniProt Gene Name	Min. E-value	Significant Pairwise Comparison		
				4D	8D	
Q802Y8	Ubiquitination	Zinc finger and BTB domain-containing protein 16-A	2.10E-99	4D	8D	
Q7Z419	Ubiquitination	E3 ubiquitin-protein ligase RNF144B	1.50E-97	4U		
Q8TB52	Ubiquitination	F-box only protein 30	2.00E-238	8D		
Q8WXK3	Ubiquitination	Ankyrin repeat and SOCS box protein 13	2.90E-09	4D		
Q2KHT6	Ubiquitination	F-box only protein 32	1.60E-131	4D	8D	
Q6TEM9	Ubiquitination	E3 ubiquitin-protein ligase MYLIP-A	3.30E-229	4D		
Q9ESN2	Ubiquitination	E3 ubiquitin-protein ligase TRIM39	2.50E-31	5U		
POCG53	Ubiquitination	Polyubiquitin-B	4.90E-93	8D		
POCG81	Ubiquitination	Polyubiquitin-H	4.10E-12	8D		
A0A0R4I9Y1	Ubiquitination	E3 ubiquitin-protein ligase rnf213-beta	0.00E+00	3D		